Glutathione Conjugated Self Assembled Gold Nanorods for the Detection of Toxic Heavy Metal Ions

A DISSERTATION SUBMITTED

BY

LAKSHMI V NAIR

IN PARTIAL FULFILLMENT OF THE REQUIREMENTS

FOR THE DEGREE OF

MASTER OF PHILOSOPHY

SREE CHITRA TIRUNAL INSTITUTE FOR MEDICAL SCIENCES AND TECHNOLOGY

THIRUVANANTHAPURAM – 695 011

DEDICATED TO

MY BELOVED FAMILY

DECLARATION

I, **LAKSHMI V NAIR**, hereby declare that I had personally carried out the work depicted in the dissertation entitled "**Glutathione Conjugated Self Assembled Gold Nanorods for the Detection of Toxic Heavy Metal Ions**" under the direct supervision of "**Dr. K. SREENIVASAN, SCIENTIST G, Laboratory for Polymer Analysis**", Biomedical Technology Wing, Sree Chitra Tirunal Institute for Medical Sciences and Technology, Thiruvananthapuram, Kerala, India.

Lakshmi

Signature

LAKSHMI V NAIR

SREE CHITRA TIRUNAL INSTITUTE FOR MEDICAL SCIENCES & TECHNOLOGY
THIRUVANANTHAPURAM – 695011, INDIA
(*An Institute of National Importance under Govt. of India with the status of University by an Act of Parliament in 1980*)

CERTIFICATE

This is to certify that the dissertation entitled **"Glutathione conjugated self assembled gold nanorods for the detection of toxic heavy metal ions"** submitted by **LAKSHMI V NAIR** in partial fulfillment for the Degree of Master of Philosophy in Biomedical Technology to be awarded by this Institute. The entire work was done by her during Aug.2009 to Aug.2010, under my supervision and guidance at Laboratory for Polymer Analysis, Biomedical Technology Wing, Sree Chitra Tirunal Institute for Medical Sciences and Technology (SCTIMST), Thiruvananthapuram-695011.

Thiruvananthapuram
Date 09-08-10

Signature
Dr.K.Sreenivasan

SREE CHITRA TIRUNAL INSTITUTE FOR MEDICAL SCIENCES & TECHNOLOGY
THIRUVANANTHAPURAM – 695011, INDIA
(*An Institute of National Importance under Govt. of India with the status of University by an Act of Parliament in 1980*)

CERTIFICATE

This is to certify that the dissertation entitled "**Glutathione conjugated self assembled gold nanorods for the detection of toxic heavy metal ions**" submitted by **LAKSHMI V NAIR** in partial fulfillment for the Degree of Master of Philosophy in Biomedical Technology to be awarded by this Institute. The entire work was done by her during Aug.2009 to Aug.2010, under my supervision and guidance at Laboratory for Polymer Analysis, Biomedical Technology Wing, Sree Chitra Tirunal Institute for Medical Sciences and Technology (SCTIMST), Thiruvananthapuram-695011.

Thiruvananthapuram
Date 09-08-10

Signature
Dr.K.Sreenivasan

The Dissertation

Entitled

Glutathione Conjugated Self Assembled Gold Nanorods for the Detection of Toxic Heavy Metal Ions

Submitted

By

LAKSHMI V NAIR

For

Master of Philosophy

Of

SREE CHITRA TIRUNAL INSTITUTE FOR MEDICAL SCIENCES AND TECHNOLOGY

THIRUVANANTHAPURAM – 695 011

Evaluated and approved

By

Signature

Name of Supervisor

Dr. K, Sreenivasan

Signature

Examiner's name and Designation

Dr. H.K. Varma
Scientist F

Acknowledgements

I express my sincere gratitude to my supervisor **Dr. K. SREENIVASAN, SIC, Laboratory for Polymer Analysis",** Biomedical Technology Wing, Sree Chitra Tirunal Institute for Medical Sciences and Technology, Thiruvananthapuram, Kerala, India for the inspiring guidance and constant support extended to me during the entire project period. It is his encouragements which lighten the difficult objectives to fulfill.

I also express thanks to **Mr. Durgadas.C.V, PhD student,** for valuable suggestions and help in laboratory. I extend my thanks to **Mr.Rowsen Mosses, Mr.Hari.P.R, Dr.Radhakumari, Mrs.Manju.S, Mrs.Vidya Raj, Mrs.Soma Deypal, Laboratory for Polymer Analysis,** Biomedical Technology Wing, Sree Chitra Tirunal Institute for Medical Sciences and Technology, Thiruvananthapuram, Kerala, India for their cooperation and support during the project periods.

I am thankful to **Dr C. P. Sharma**, **SIC**, **Biosurface Technology Division,** and **Dr. Annie John**, **SIC**, **TEM Division,** Biomedical Technology Wing, Sree Chitra Tirunal Institute for Medical Sciences and Technology, Thiruvananthapuram, Kerala, India for the instrumental support for the study.

I am thankful to **Dr. Lizzy K. Krishnan, Scientist G, Thrombosis Research Unit**, **Dr. Jayasingh, Deputy Registrar, and Division of Academic Affairs** Biomedical Technology Wing, Sree Chitra Tirunal Institute for Medical Sciences and Technology, Thiruvananthapuram, Kerala, India for the valuable guidance and help throughout this course.

I am thankful to The **Head**, **BMT wing** and the **Director (SCTIMST)** for the fellowships and facility.

I thank all my friends, seniors and relatives who have rendered direct or indirect help during the course of this project work.

Above all, I thank the almighty for all the good things happened in my life.

Table of Contents

List of Figures

List of Scheme

ABBRIVATIONS

QDs	Quantum Dots
SWCNT	Single Walled Carbon Nanotubes.
GNRs	Gold Nanorods.
LSPR	Localized Surface Plasmon Resonance.
EM	Electromagnetic
PDT	Photo Dynamic Therapy
GSH	Glutathione
AR	Aspect Ratio.
GSH GNR	Glutathione functionalized Gold nanorod
SPR	Surface Plasmon Resonance.
TPRS	Two photon Rayleigh scattering
Cfu	Colony forming unit
TPL	Two Photon Luminescence
TPAF	Two photon auto fluorescence
NLO	Nonlinear optical
HRS	Hyper -Rayleigh scattering
NIR	Near Infra Red
EGFR	Epidermal Growth Factor Receptor
CTAB	N-CetyltrimethylAmmonium bromide.

DSA	Directed Self Assembly.
PAA	Poly(acrylic acid)
MS	Mesoporous silica shell
DI	Deionised
AA	Ascorbic Acid.
FTIR	Fourier Transform Infra Red Spectroscopy.
DTGS	Deuteriated Triglycine Sulphate.
DLS	Dynamic Light Scattering.
HRTEM	High Resolution Transmission Electron Microscope.

Synopsis

The Interdisciplinary science “nanoscience” has many applications in most of the fields, which were directly linked to human’s daily life. Nanobiotechnology and nanomedicine are the emerging science from the contribution from multiple scientific areas. Nanomedicine defines the applications of nanomaterials in safer environments for better results in biological applications.

Chapter 1 of the report makes a brief introduction and review of literature about the area of interest. Based on the review of literature a research objective has formulated. The potential applications of nanoscience in biological aspects include the diagnostic purpose (sensors and markers), cellular imaging, therapeutics, drug delivery etc. The relevance of nanomaterials is that the individual nanoparticles have properties which are distinct from those of bulk. As the dimension of materials are so small, any factor which affects dimension either directly or indirectly will reflects in its optical properties. This will enable one to make a highly sensitive senor or a diagnostic tool for many applications.

Properties of nanomaterial can be tailored by self assembly (a process of patterning the materials in to one direction by virtue of its internal factors and were not caused by an external force) or by proper engineering the material surface. Nanomaterials exhibit highly tunable physicochemical behavior when allowed them to self assembles in 2D or in 3D. Among the most studied nanostructures, materials of inorganic origin were found to be more useful in many applications. The most explored materials for the above mentioned applications includes Quantum Dots (QDs), nano colloids of noble metals (mainly gold and silver) and nanotubes (single walled carbon nanotubes, SWCNT) . Among them, the gold colloids are versatile structures having more beneficial in biological applications due to their less toxic nature compared to other materials. Recent reports shows biological applications such as sensing in vivo cellular imaging can be performed with gold nanostructures. Researchers have developed many preparatory methods either physical or wet chemical approaches for generating various gold nanostrutures like spheres, rods, cubes, tetrahedral etc. Each structure showed some superior qualities over other structures originated from the same element, gold.

Gold nanorods (GNRs) attracted the attention of both the researchers from nanobiotechnology and nanotechnology because of their peculiar optical property (Localized Surface Plasmon Resonance, LSPR). Gold colloids exhibited visible light absorbance in electromagnetic spectrum (EM) compared to bulk gold. But GNRs have two absorption bands one in visible and the other tunable from visible to IR region in the EM spectrum. The first absorption band which usually have less amplitude will be around 520 nm called as the transverse band and the other which is tunable usually >600nm called as the longitudinal band. The latter one is more sensitive to the environments. There were many reports available based on colorimetric as well as LSPR techniques for sensing and diagnostic applications. But the applications based on gold nanorods which are useful in cancer cell killing (Photo Dynamic Therapy, PDT), cancer marker, sensor in various detection and diagnostic purpose are in an emerging stage. Moreover research has directed in assembling the gold nanorods for improved optical and chemical characteristics. There were many methods available for assembling gold nanorods either end to end fashion or to side by side. To the best of our knowledge the assembly disassembly technique in gold nanorods has not been used for any selective sensor applications. This report focuses to study the role of entities which could disassemble chain like formation of gold nanorods and to design new sensing methodologies.

Chapter 2 of the report discusses materials and methods of this study. This includes a brief theory and principle of various instruments used in the study. The study used UV/ Visible, DLS, FTIR and HRTEM as the major instruments for characterization. The wet chemical approaches to gold seed synthesis and gold rod synthesis were elaborated in the experimental section. Thus synthesized gold nanorods were functionalized with glutathione (GSH) and Cysteine.

Chapter 3 includes the results and discussions. The present report studied disassembling the end to end assembled gold nanorods with cations. We could be able to make gold nanorods with tunable aspect ratio AR by varying three conditions like temperature of the reaction, concentration of seeds and concentration of reducing agents. The smaller gold nanorods showed very good batch to batch reproducibility, keeping the reagents concentrations same in all experiments. Assembly of gold nanorod was achieved through amino acids glutathione and L- cysteine as per the previous reports. This assembly was characterized by UV-Visible spectroscopy, HRTEM and Dynamic Light Scattering (DLS). Self assembled chain structures of gold nanorods were found to be selectively broken or disassembled in presence of heavy metal ion, lead and copper enabling the use of nanorods for the sensing of ions such as Pb. The disassembly was also confirmed in HRTEM and DLS analysis. We found that DLS is also a good instrumental technique to evaluate the variation in the nano assembly for sensor applications.

Conclusion of the results in chapter 4 summarizes the synthesis of gold nanorods with tunable aspect ratio, its end to end assembly and selective disassembly. The study reveals that the GSH GNR was selectively disassembled in presence of lead where as cysteine GNR disassembled in the presence of copper. The selectivity of metal ions in presence of other cations was also tested as the control experiment. The method described in this project seems to have potential to be used as selective sensing of lead and copper.

CHAPTER 1

INTRODUCTION

CHAPTER 1

INTRODUCTION

1.1 Introduction

The present era of scientific research made significant attention on the applications of Nanoscience and Nanotechnology. This interdisciplinary area of science got significance after the well celebrated talk of Richard P. Feynman (Nobel Laureate in physics-1965) “There's Plenty of Room at the Bottom”, at the annual meeting of American Physical Society at California Institute of Technology, on December 29th 1959. The talk focused on miniaturization of materials which may be able to solve many scientific problems that exist. The nanoscience deals with the manipulation over material, creating various properties. The Nanoscience to technology was developed later and the term was coined by Prof. Norio Taniguchi and Prof. K Eric Drexler, which discuss the applications of nanomaterials. One nanometer is one billionth, 10^{-9} of a meter. The well accepted definitions of nanomaterial are materials where the size of the individual building blocks is less than 100 nm. Nanomaterials may be zero dimensional (spherical nanoparticle), one dimensional (nanorod or nanotubes) or two dimensional (film or stack of thin film).

Usually chemistry synonyms the nanoscience as it deals with manipulation of material properties in atomic scale. Nanoparticles are number of atoms or molecules bonded together (these particles usually contain 10^6 atoms or fewer) and are intermediate in size between individual atoms and aggregates large enough to be called bulk material. As nanoparticles are much larger than individual atoms and molecules but are smaller than bulk solid materials, their behavior is in between that of a macroscopic solid and that of an atomic or molecular system. There are three major factors responsible for these differences

- High surface to volume ratio.
- Quantum size effect.
- Electrodynamics interaction.

Metallic nanoparticles show unique optical, electronic, chemical and magnetic properties that were entirely different from that of bulk materials. Colloidal solutions of gold, copper, silver etc show characteristic color in visible light. Compared to bulk gold which has a yellow color, caused by a reduction in reflectivity for light at the end of the spectrum, the colloidal gold showed a bright wine red color caused by the free surface electrons at the nanoparticle surface. Among the noble metals gold has attracted human in all time. The extraction of gold started in the 5th millennium B.C. in Bulgaria, "soluble" gold appeared around the 5th century B.C. in Egypt and China. The Lycurgus cup (4th century A.D), which can be seen at the British Museum, is a striking example of the early (artistic) use of metal nanoparticles embedded in glass: the vessel appears green in daylight (reflected light), but red when it is illuminated from the inside (transmitted light). Paracelsus described the preparation of potable gold, which was believed to have remarkable medicinal properties. Until the middle Ages, the soluble gold was used to disclose fabulous curative powers for various diseases, such as venereal problems, dysentery, epilepsy, and tumors, and for diagnosis of syphilis. Thus, the remarkable features exhibited by colloidal gold have been utilized for centuries.

Importance of colloidal gold is that, the general resonance frequency lies in the visible and near IR region and gold is one of the metal nanoparticles noble enough to survive as nanoparticles under atmospheric conditions. Characteristically, noble metal nanoparticles exhibit a strong absorption band in the visible region, and this is indeed a small particle effect, since these are absent in the individual atom as well as in the bulk. The physical origin of light absorption by metal nanoparticles is the coherent oscillation of the conduction band electrons induced by the interacting electromagnetic field. The oscillation modes comprise an electromagnetic field coupled to the oscillations of conduction electrons and are called surface plasmons. An absorption band results when the incident photon frequency is resonant with the collective oscillation of the conduction band electrons and is known as the surface plasmon resonance (SPR).

The resonance frequency of this SPR is strongly dependent upon the size, shape, interparticle interactions, dielectric properties and local environment of the nanoparticle. Researching in gold nanomaterials provides platforms for exploring the same for many biological and optical applications.

1.2 Review of Literature

The Localized Surface Plasmon Resonance (LSPR) property [Kerke M; 1969, Bohren & Huffman; 1983] of noble metal nanomaterials results from strong interaction with light makes them an attractive nanostructure in nanoscience and technology. Based on the quantum mechanical approach, it is assumed that the electrons in the metal behave as a wave having certain energy. When light falls on this materials the photons of the light is absorbed by the electron cloud creating a resonance condition. The photon absorbed by the material dissipates energy by the oscillation of electron wave resulting in plasmon. As the process occurs at the surface of the metals it is called Localized Surface Plasmon Resonance. When the wavelength of light is much larger than the nanoparticle size it can set up standing resonance conditions **(scheme 1).**

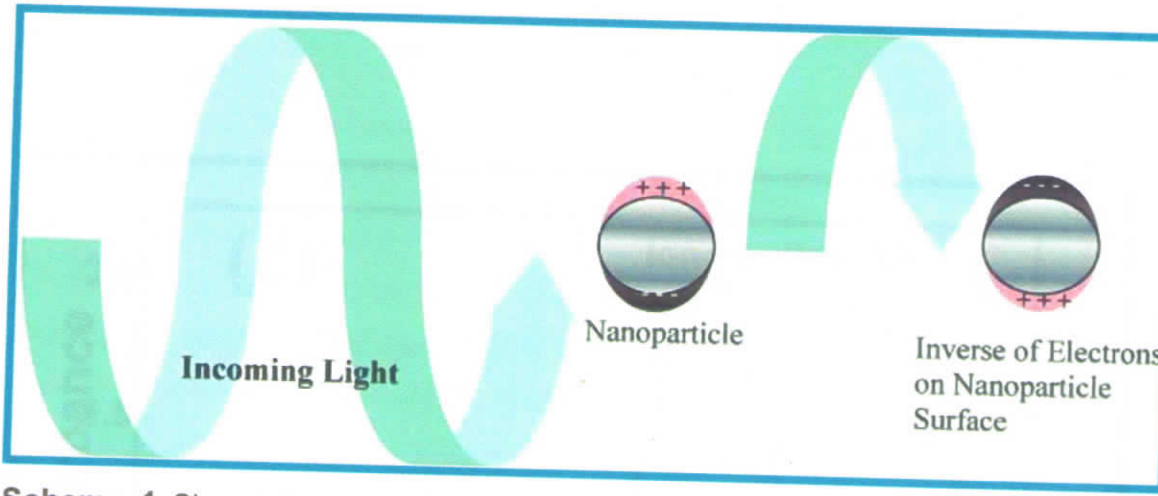

Scheme 1 Shows the resonance condition between the metal surface and incident photons. [Eustis S & El-Sayed M. A.; 2006]

LSPR is also influenced by size and shape of the nanomaterial. Tuning the LSPR by controlling the size and shape of noble metal nanomaterials especially gold, has gained much attention in recent periods.

Murphy et al. and El-Sayed et al. have extensively studied the parameters of synthesis of noble metal nanostructures for various applications. Studies showed that the size and shape variation in gold nanomaterials will alter their physicochemical behavior [Jain et al.; 2006, El- Sayed MA; 2001, Link S & El-sayed MA; 2000, Link S & El-sayed MA; 1999.]. Among the various nanostructures of gold, the nanorods are versatile structures attracted the attention of material scientists due to their special LSPR. Gold nanorods (GNRs) have two directional electron oscillations in response to the polarization of incident light. One will be along the length (longer axis) and the other along the breadth (shorter axis) of the nanorods. The absorbance along longer axis was always exhibited a strong absorption (usually > 600nm) which is referred to as the longitudinal band and the shorter axis one (around 520nm) is called the transverse band. LSPR shows significant changes with respect to the variation in the aspect ratio (length/breadth).

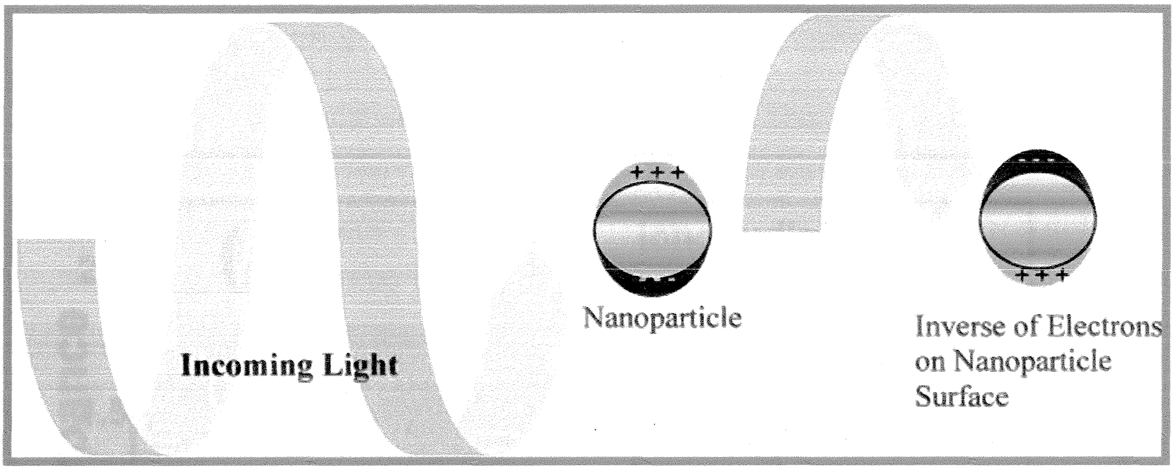

Scheme 1 Shows the resonance condition between the metal surface and incident photons. [Eustis S & El-Sayed M. A.; 2006]

LSPR is also influenced by size and shape of the nanomaterial. Tuning the LSPR by controlling the size and shape of noble metal nanomaterials especially gold, has gained much attention in recent periods.

Murphy et al. and El-Sayed et al. have extensively studied the parameters of synthesis of noble metal nanostructures for various applications. Studies showed that the size and shape variation in gold nanomaterials will alter their physicochemical behavior [Jain et al.; 2006, El- Sayed MA; 2001, Link S & El-sayed MA; 2000, Link S & El-sayed MA; 1999.]. Among the various nanostructures of gold, the nanorods are versatile structures attracted the attention of material scientists due to their special LSPR. Gold nanorods (GNRs) have two directional electron oscillations in response to the polarization of incident light. One will be along the length (longer axis) and the other along the breadth (shorter axis) of the nanorods. The absorbance along longer axis was always exhibited a strong absorption (usually > 600nm) which is referred to as the longitudinal band and the shorter axis one (around 520nm) is called the transverse band. LSPR shows significant changes with respect to the variation in the aspect ratio (length/breadth).

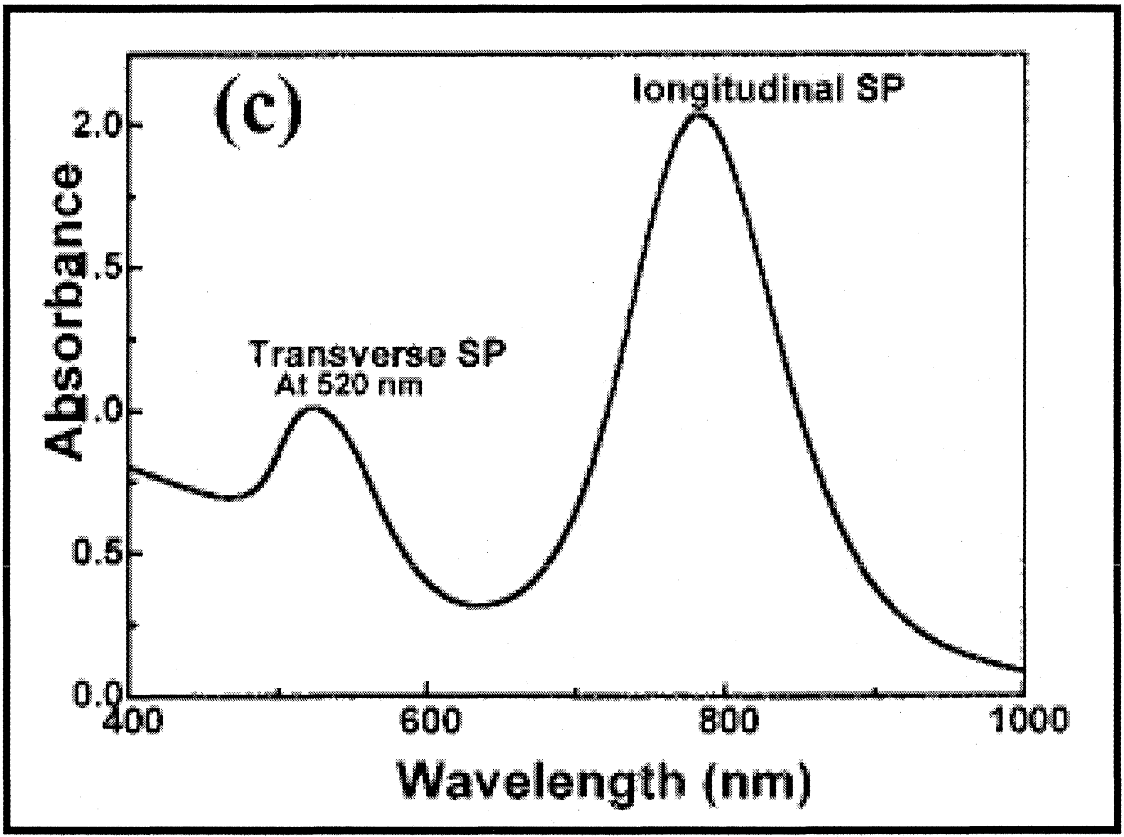

Figure 1 A typical SPR of the gold nanorods. (Jain et al.; 2006, El- Sayed MA; 2001, Link S & El-sayed MA; 2000, Link S & El-sayed MA; 1999.)

Moreover the stronger absorption band (longitudinal) was much more sensitive to the environment of the system [Marzan LML; 2004, Jain PK et al.; 2007.]. This feature enables the GNR as good plasmonic material in sensing and optical applications.

1.2.1 Applications of gold nanorods

Gold Nanorods were widely used for drug targeting, photothermal agent, Contrast agent for biological imaging, Sensing etc. Functionalizing the nanorod with appropriate ligand made it possible for this application. Gold nanorod can convert optical energy into heat via non radiative electron relaxation dynamics, endowing them with intense photo thermal therapy. The recent applications of the gold nanorods includes multiplex biosensor [Yu C, Irudayaraj J; 2007] cancer cell imaging in NIR regions [Huang X et al.; 2006] hyperthermia agents in cancer photodynamic therapy [Kuo WS et al.; 2010] etc. All the above applications are mainly dependant on the aspect ratio of the rod. So controlling the growth of rod size is an important step in selecting the material for a particular application.

Singh et al. studied Two-photon Rayleigh scattering (TPRS) properties of gold nanorods for rapid, highly sensitive and selective detection of Escherichia coli bacteria from aqueous solution, without any amplification or enrichment in 50 colony forming units (cfu)/mL level with excellent discrimination against any other bacteria. TPRS intensity increases 40 times when anti-E.coli antibody-conjugated nanorods were mixed with various concentrations of Escherichia coli O157:H7 bacterium. This bionanotechnology assay could be adapted in this study using antibodies specific for various bacterial pathogens for the detection of a wide variety of bacterial pathogens used as bioterrorism agents in food, clinical samples, and environmental samples. [Singh AK et al.; 2009]

The reports of Hauck et al. [Hauck TS et al.; 2008] showed that combining hyper thermia effects caused by gold nanorods with chemotherapy will improve the toxicity to cancer cells with selectivity. This report has benefits compared to the present hyperthermia methods where the whole body is being heated without any selection by external source. Also combining with the chemotherapy agents, a synergic or superadditive toxicity has offered to the cancer cells.

Nicholas et al. demonstrated the use of gold nanorods as bright contrast agents for two-photon luminescence (TPL) imaging of cancer cells in three dimensional tissue phantom down to 0.075 mm deep. [Durr JN et al.; 2007] The TPL intensity from gold-nanorod-labeled cancer cells is three orders of magnitude brighter than the two-photon auto fluorescence (TPAF) emission intensity from unlabeled cancer cells at 760 nm excitation light. The strong signal, resistance to photobleaching, chemical stability, ease of synthesis, simplicity of conjugation chemistry, and biocompatibility make gold nanorods an attractive contrast agent for two-photon imaging of epithelial cancer.

Darbha et al. reported the second-order nonlinear optical (NLO) properties of gold nanorods can be used for screening HIV-1 viral DNA sequence without any modification, with good sensitivity (100 pM) and selectivity (single base-pair mismatch). [Darbha GK et al.; 2008]The hyper-Rayleigh scattering (HRS) intensity increases 45 times when a label-free 145 mer, ss-gag gene DNA, was hybridized with 100 pM target DNA. The mechanism of Hyper Rayleigh scattering intensity change has been discussed with experimental evidence for higher multipolar contribution to the NLO response of gold nanorods.

Xiaohua et al. showed that anti-epidermal conjugated gold nanorod can selectively kill the cancer cell because of the emission in the NIR region. Gold nanorods with suitable aspect ratios can absorb and scatter strongly in the NIR region (650-900 nm). In this work they also provide an in vitro demonstration of gold nanorods as novel contrast agents for both molecular imaging and photothermal cancer therapy. Nanorods were synthesized and conjugated to anti-epidermal growth factor receptor (anti-EGFR) monoclonal antibodies and incubated in cell cultures with a nonmalignant epithelial cell line (HaCat) and two malignant oral epithelial cell lines (HOC 313 clone 8 and HSC 3). The anti-EGFR antibody-conjugated nanorods bind specifically to the surface of the malignant type cells with a highest affinity due to the over expressed EGFR on the cytoplasmic membrane of the malignant cells. As a result of the strongly scattered red light from gold nanorods in dark field microscope the malignant cells are clearly visualized and diagnosed from the nonmalignant cells. After exposure to continuous red laser at 800 nm, malignant cells require about half the laser energy to be photothermally destroyed than the nonmalignant cells. Both efficient cancer cell diagnostics and selective photothermal therapy are realized at the same time. [Huang X et al.; 2006]

Norman et al. showed that Antibody conjugated gold nanorod can be used to selectively target pseudomonas aeruginosa cells and also considerably reduces the cell viability. [Norman RS et al.; 2008] Increases in the prevalence of antibiotic resistant bacteria require new approaches for the treatment of infectious bacterial pathogens. Nanotechnology-driven approach was used to selectively target and destroy pathogenic bacteria. They explored this approach using gold nanorods. Gold nanorods were covalently linked to primary antibodies to selectively destroy the pathogenic Gram-negative bacterium, Pseudomonas aeruginosa. Nanorod attachment to the bacterial cell surface, exposure to near-infrared radiation results in a significant reduction in bacterial cell viability.

1.2.2 Synthetic methods

A number of approaches for the gold nanorod synthesis were available which includes electrochemical method, Photochemical and wet chemistry approach or seed mediated synthesis.

1.2.2.1 Electrochemical method: In this method [Yu Y et al.; 1997, Chang SS et al.; 1999] a gold plate used as anode and platinum plate as cathode. The electrolyte used was a cationic surfactant hexadecyltrymethylammonium bromide (CTAB), which plays dual role as a electrolyte and capping agent. Within the electrolyte solution the bulk gold converted in to nanoparticles at the cathodic interface. The growth of cylindrical gold nanorods were done by controlling the current and voltage to an optimum value and the process was initiated by addition of acetone.

1.2.2.2 Photochemical: Here the capping was done with a mixture of CTAB and tetradodecylammonium bromide growth solution [Esumi K et al.; 1995, Kim F et al.; 2002, Leontidis E et al.; 2002]. In presence of cyclohexane and acetone the gold chloride (precursor for rod growth) were reduced to gold nanorods by UV of wavelength 254 nm, irradiation for 30 hrs. The Silver nitrate was a requirement for the process.

1.2.2.3 Wet Chemistry approach: The seed mediated synthesis developed and modified by Murphy et al. [Jana NR et al.; 2001, Jana NR et al.; 2001, Johnson CJ et al.; 2002, Murphy CJ et al.; 2005] is the most accepted and easy wet chemical approach for the gold nanorod synthesis. In this method GNRs were prepared by a two step approach. The rods were grown by the addition of citrate-capped small gold nanospheres, called as seed solution, to a bulk $HAuCl_2$ growth solution obtained by the reduction of $HAuCl_4$ with ascorbic acid in the presence of cetyltrimethylammonium bromide (CTAB) surfactant and silver ions. The approach was later modified by Nikoobakht et al [Nikoobakht B & El-Sayed MA; 2003] to get high yield monodisperse GNRs. Later many studies have performed to investigate the roles of various components in controlling the aspect ratio of the gold nanorods [Gole A & Murphy CJ; 2004, Sau TK & Murphy CJ; 2004]. These studies revealed that the size and concentration of the seed solution, concentration of ascorbic acid, concentration of the silver ions, surface chemistry of the seed etc has direct influence in controlling the aspect ratio of the gold nanorods. Concluding all these studies shows that the surfactant CTAB caps preferentially adsorbs to their {1, 1, 0} and {1, 0, 0} side faces. The attachment of CTAB to the {1, 1, 1} side faces is weak where the growth of the rod proceeds [Wang ZL et al.; 200]. This reveals that the {1, 1, 1} side face can be used for attaching chemical linkers for the further exploration of the plasmonic material.

1.2.3 Assembling gold nanorods

The self assembly as mentioned above refers to the spontaneous alignment of the structures by virtue of its internal interactions. In the area of nanoscience self assembly of nanostructures can create novel structures with predictable properties. Here the term of 'bottom up nanofabrication' means a controlled linking of nanostructures without allowing them to aggregate has significance. A recent review [Grzelczak M et al.; 2010] discusses the importance of the directed self assembly (DSA) in nanoparticles for various applications. There were reports available for the vertical alignments and lateral alignments of colloidal nanorods by making use of various interactions like Vander Waals interaction. But the end to end connection was a challenge. But for gold nanorods as stated above the growth tip or end is usually not covered by the surfactant and can be use for end to end assembly. This feature was well explored for interconnecting the gold nanorods end-end assembly for tuning the surface plasmon for optical applications by a process called plasmon coupling.

The area got much attention when Murphy et al. [Caswell KK et al.; 2003] in 2003 reported the end to end GNR self assembly in biotin functionalized GNRs in presence of streptavidin linker. The affinity for the biotin, a small biomolecule towards the protein streptavidin is well known. The protein can bind with four molecules of the biotin molecule. Here the biotin disulphide molecules are allowed to self assemble over GNR resulting a monolayer of the biotin. Another set of gold GNRs were then coated with streptavidin. The Streptavidin coated gold nanorods were then titrated against the biotin coated rod results in the end to end assembled chain of gold nanorods.

After this first report Thomas et al [Thomas KG et al.; 2004] proposed the uniaxial coupling phenomenon in GNRs through the longitudinal self assembly based on the mercaptocarboxylic acid linkages. The linkage longitudinal assembly was achieved by a cooperative intermolecular hydrogen bonding offered by the carboxylic acids. Later the gold nanorod aggregation induced by the streptavidin-biotin binding was reported [Gole A & Murphy CJ; 2005] using the polymer coated side by side alignment process also. Here the aggregation of gold nanorods was produced by making an entire coating over GNR with biotin. In the first step the GNRs were coated with poly (acrylic acid), PAA and the amine end of the biotin was connected to acid part of PAA by carbodiimide chemistry. Then the addition of the streptavidin resulted the binding over the entire region of the rod and finally aggregated through the interconnectivity. A selective detection method in the micromolar level for glutathione and cysteine aminoacids were also suggested by Thomas et al. [Sudeep PK et al.; 2005] by an interplasmon coupling by the hydrogen bonding in the aminoacid which shifts the longitudinal plasmon band without affecting the transverse band.

Jain et al. [Jain PK et al.; 2006] suggested the exciton-coupling model for the plasmon coupling in GNRs. The recent applications of GNR are mainly based on the self assembly. The self assembly of GNRs to one-, two-, and three-dimensional structures observed previously [Nikoobakht B et al.; 2000] depending on the nanoparticle concentration, solvent evaporation, narrow size distribution, ionic strength, and surfactant concentration of the parent solution. The same authors also observed the ability of cancer cells to self assemble the antibody conjugated gold nanorod, as a cancer marker candidate [Huang X et al.; 2007].

The mechanistic aspects of the gold nanorod chain formation were studied using a, ? -alkanedithiols by [Joseph STS et al.; 2006]. The report shows that after a critical concentration of the dithiols the longitudinal surface plasmon decreases and red shifted. This is attributed to the interplasmon coupling. Based on this investigation the possible mechanisms of chain formation were suggested.

Initially the alkane dithiols binds with the edges of the gold nanorods leaving one thiol group free. As concentration changes the dimmers were resulted. Thus formed dimmers start to grow to oligomers and later to rod chain. Possibilities of chain formation were shown schematically (**scheme 2**) as follows.

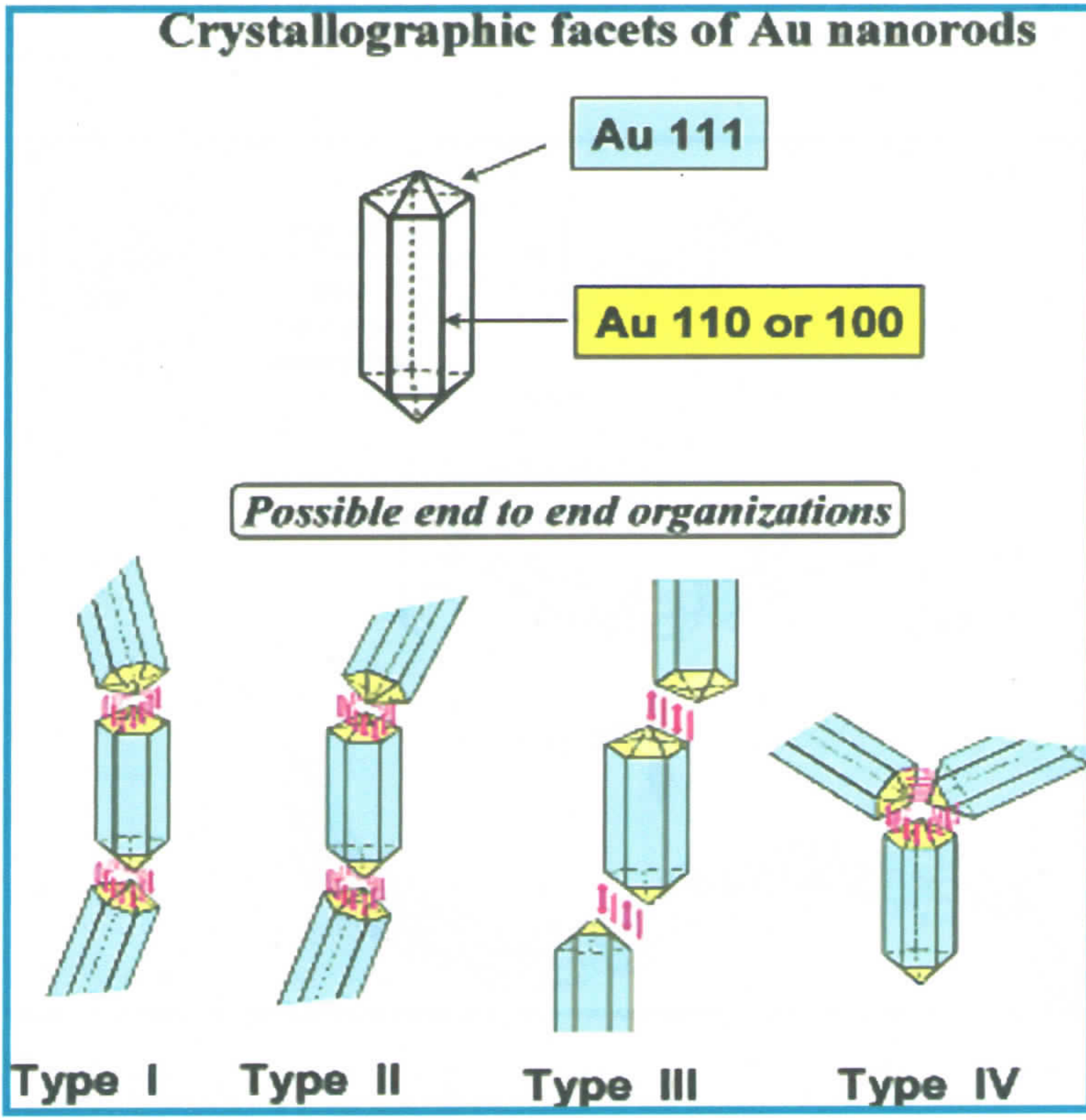

Scheme 2 Crystallographic facets of gold nanorods participating in the gold chain formation (Joseph STS et al.; 2006).

According to the seed mediated gold nanorod synthesis as described above, the mechanism of the gold nanorod formation is by the anisotropic growth along the {111} edges. The growth along crystallographic facets of Au nanorod ({100} or {110} was blocked by the surfactant molecules usually CTAB. The oligomer to chain growth above the critical concentration of the dithios has schematically shown below (**scheme 3**).

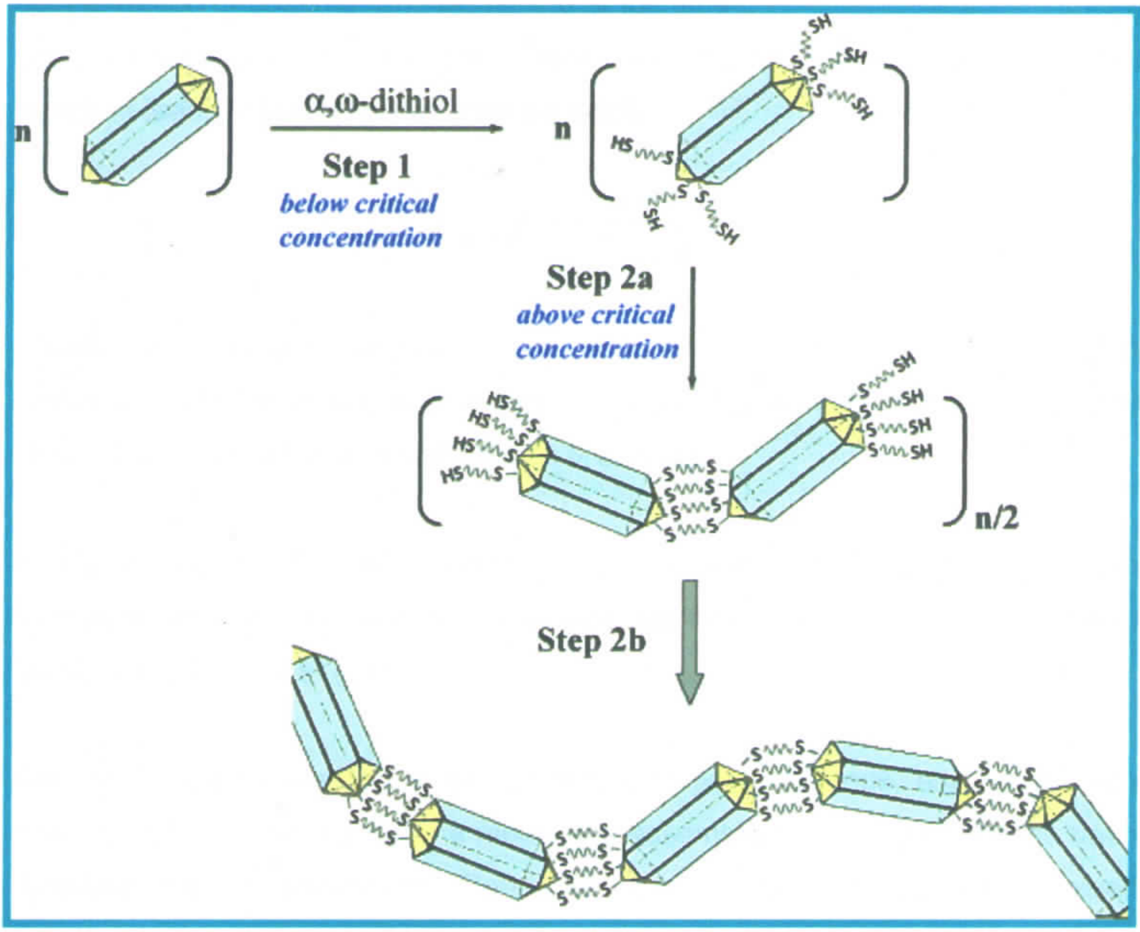

Scheme 3 Shows the schematic representation of the process of gold nanorod to dimer-oligomer and finally chain formation in presence of α, ω-alkanedithiols((Joseph STS et al.; 2006)).

The dimer – oligomer leading to chain is believed to be a follow a second order kinetics as per the following equation

$$k_{\text{dimer}}t = \frac{x}{a_0(a_0 - x)}$$

Where the k_{dimer} represents the second order rate constant for dimer formation, x is the concentration of the gold nanorod reacted in time t and $a_0 - x$ is the concentration of gold nanorod remaining at the time t.

Up on substitution of the concentration and further derivation of the above equation leads to the simplified form as below

$$k_{\text{dimer}}t = \frac{\epsilon(A_0 - A_t)}{A_0 A_t}$$

Where A_0/e initial concentration of gold nanorod, A_0- A_t/e, concentration of gold nanorod reacted in time t, A_t/e as concentration of gold nanorod remaining after time t. The A_0 and A_t are absorbance at t_0 and at t.

Based on the above kinetic studies it is proposed that the gold nanorod chain formation proceeds through an incubation period-dimerisation- oligomerization and finally the chain of gold nanorod.

Recent reports showed an in situ assembly of gold nanorods, end-to-end, into long chains attached on top of a mixed self-assembled monolayer that has been functionalized with streptavidin [Zareie MH et al.; 2007]. Another report showed that the thiol polymer terminated gold nanorod will self assemble to give various block nanostructures [Fava D et al.; 2008].

1.2.4 Sensor applications based on gold nanostructures

Chang et al. reported orientation of GNRs induced by bioregonition [Chang JY et al.; 2005]. In the report thioctic acid molecules conjugated gold nanorods were grown to linear chains in the presence of mouse IgG. The report shows the feasibility of using GNRs to study the antigen-antibody recognition. During our studies an Wang et al. [Wang L et al.; 2010] reported the use of side by side and end to end assembled gold nanorods for the sensing of the environmental toxin microcystin.

Stella et al. reported that suitably functionalized gold nanorod can be used for the detection of model analyte in serum. Gold nanorods were chemisorbed onto a mercaptosilane-modified glass substrate, followed by conjugation of biotin to the nanorods. Streptavidin binding to biotin was monitored by the wavelength shift of the local surface plasmon resonance peak in the UV-VIS extinction spectrum of the immobilized gold nanorods due to the change in local refractive index at the gold nanorod surface induced by streptavidin binding. The limit of detection of the sensor is 0.005 μg/mL (94 pM) in PBS and 1 μg/mL (19 nM) in serum, and the dynamic range spans 94 pM to 0.19 μM. The advantages of the nanorod based sensor over a local surface plasmon resonance sensor from gold nanospheres are the significantly lower detection limit and the internal self reference that the signal of the nanorod sensor provides based on the measurement of peak wavelength shift. [Marinakos SM et al.; 2007]

Wu et al. studied the Core-shell structured Gold nanorods with a surface-exposed gold core and a mesoporous silica shell (MS Gold nanorod) were demonstrated as a promising platform for localized surface plasmon resonance based molecular sensing. Mesoporous silica shell not only allows the gold nanorod's core to be directly exposed to their surrounding environment but also stabilizes the dispersion in various water-organic mixtures and pure organic solvents. The local surface plasmon resonance bands of mesoporous silica Gold nanorods displays a stable and linear response in spectral shift to the changes in their surrounding refractive index with a sensitivity of325nm/RIU. To demonstrate the application of mesoporous silica nanorod as local surface plasmon resonance nanosensors in molecular sensing, the plasmon response to molecular adsorbates (GSH) was demonstrated. Mesoporous silica gold nanorods provide a more stable and sensitive response than CTAB-capped Gold nanorod in GSH sensing. In addition, they demonstrated that the local surface plasmon resonance response of Gold nanorod is highly sensitive to changes of local refractive index in mesoporous silica shell, which renders the feasibility of using mesoporous silica Gold nanorod as effective molecule-sensing platforms when mesoporous silica shells were functionalized with various chemical and biological ligands. [Wu C & Xu QH; 2009]

Nusz et al.reported the use of individual gold nanorods as Plasmonic transducers to detect the binding of streptavidin to individual biotin-conjugated nanorods in real time on a surface. Label-free detection at the single-nanorod level was performed by tracking the wavelength shift of the nanorod-localized surface plasmon resonant scattering spectrum using a dark-field micro spectroscopy. The lowest streptavidin concentration that was experimentally measured was 1 nM, which is a factor of 1000- fold lower than the previously reported detection limit for streptavidin binding by biotinylated single Plasmonic nanostructures. Binding of streptavidin at 1 nM concentration induces a mean resonant wavelength shift of 0.59 nm. [Nusz GJ et al.; 2008]

Yu et al. studied gold nanorods with different aspect ratios fabricated through seed-mediated growth and surface activation by alkanethiols for the attachment of antibodies to yield gold nanorod molecular probes. Multiplex sensing was demonstrated by the distinct response of the plasmon spectra of the gold

1.3 Present status

The literature review showed that there were methods available for assembling the gold nanorods but limited reports for reversing the same. To the best of our knowledge the assembly- disassembly technique in gold nanorods has not been used for any selective sensor applications.

1.4 Objectives of the present work

The objectives of the present project confine to study the nature of amino acids induced assembly of gold nanorods and the role of heavy metal ions such as lead (Pb) in disrupting the assembled structures. The programmer's another objective is to demonstrate the analyte induced disassembly as new approach for sensing.

CHAPTER 2

MATERIALS AND METHODS

CHAPTER 2

MATERIALS AND METHODS

2.1 Materials used

All the experiments were carried out in deionised (DI) water and glass wares were cleaned with aqua regia *(Aqua regia is toxic and care should be taken while handling)*. All the reagents were used as supplied without further purification until and unless stated. Gold (III) chloride trihydrate, L-Cysteinehydrochloride monohydrate, N-Cetyltrimethylammoniumbromide,CTAB and sodium Borohydide were obtained from Sigma-Aldrich, Bangalore, India. Glutathione reduced was from SRL, Mumbai, India. Silver Nitrate, L- Ascorbic Acid, Lead Acetate, Zinc nitrate hexahydrate, Mercuric chloride, Nickel chloride, Cobalt chloride, Cadmium chloride, Manganese chloride and copper Sulphate pentahydrate were from MERCK, Mumbai, India.

2.2 Instrumental Techniques

UV Carry 100 Bio (Melbourne, Australia) was used for measuring the absorbance of samples. FTIR Nicolet 5700 (Madison, USA) with Deuteriated Triglycine Sulphate(DTGS) detector was employed for characterizing the chemistry of the materials in each modification, Malvern Zeta sizer Nano ZS (UK) equipped with a laser power of 633 nm was used for hydrodynamic size measurements. HRTEM, Hitachi (Tokyo, Japan) 76500 (110kV) was used for viewing the nanomaterials.

2.2.1 UV Visible Characterization

UV visible spectroscopy is an absorbance spectroscopy in the UV- visible region of electromagnetic spectrum. In this region the molecule undergo electronic transition from ground state to the excited state by absorbing definite amount of energy. Measurement of the absorption of UV and visible radiation by species in solution is one of the most widely used methods of qualitative and quantitative analysis. This is complimentary to fluorescence spectroscopy. [Denney RC & Sinclair R; 1987.]

Principle: Basic principle of uv visible spectrophotometer is Beer- Lambert's law. The law states that the absorbannce of a material is directly proportional to the concentration of the solution and the path traversed by the light. That is

$$A \; a \; c^{*} \, l.$$

$$A \; a \; e^{*} \, c^{*} l.$$

$$\log I / I_0 = e^{*} \, c^{*} l.$$

Where I & I_0 are the intensity of transmitted light & incident light respectively

A is the Absorbance of the material

C is the concentration of the sample.

l is the path length.

e is the molar absorptivity coefficient.

CARRY 100 Bio is a double beam spectrophotometer. Software used is varian version 4.05.

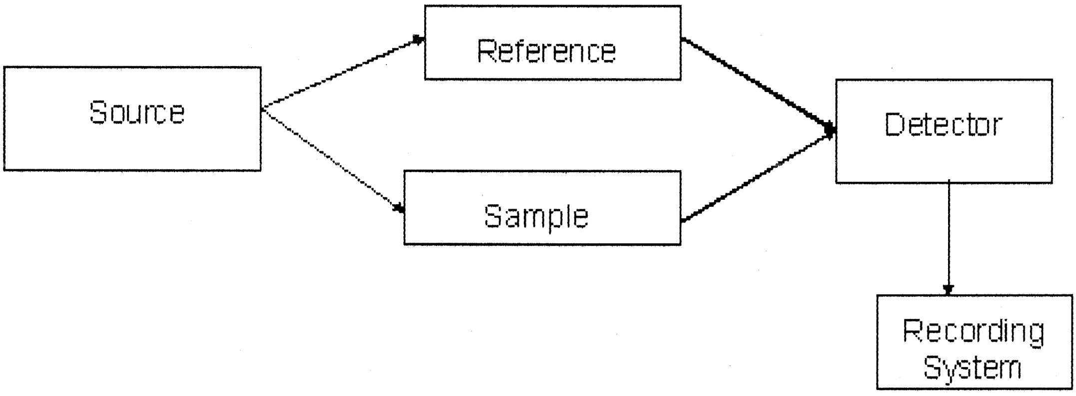

Block diagram representing double beam UV/ Visible Spectrophotometer [Carry 100 Bio (Melbourne, Australia)]

2.2.2: FOURIER TRANSFORMS INFRARED SPECTROSCOPY:

In infrared spectroscopy, IR radiation is passed through a sample. Some of the infrared radiation is absorbed by the sample and some portion transmitted. The resulting spectrum represents the molecular absorption and transmission, creating a molecular fingerprint of the sample. The term Fourier Transform Infrared Spectroscopy (FTIR) refers to a fairly recent development in the manner in which the data is collected and converted from an interference pattern to a spectrum. A molecule is said to be IR active if there is a change in dipole moment. [Banwell CN & Mc Cash EM; 1994.]

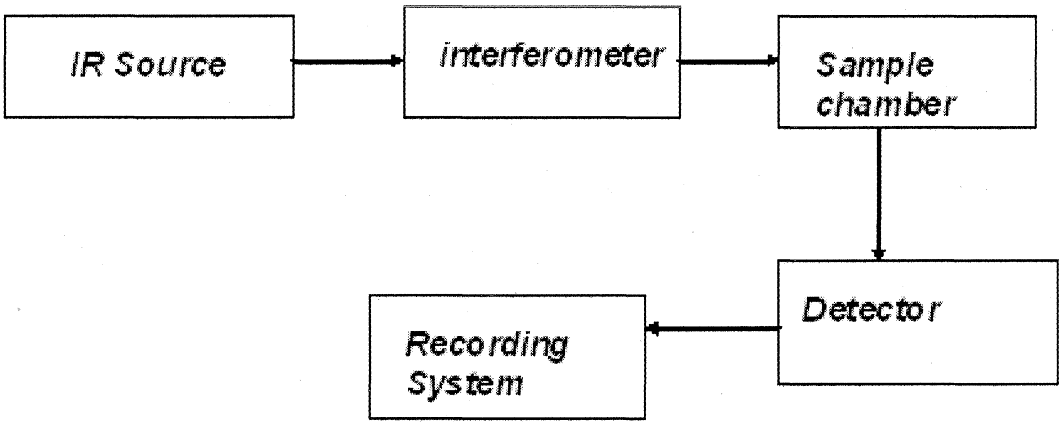

Block diagram representing FTIR [Nicolet 5700 (Madison, USA)]

In Nicolet 5700 FTIR software used is Omnic 7.3.

2.2.3 Dynamic Light Scattering

Dynamic Light scattering (DLS), also known as Photon Correlation Spectroscopy (PCS) and is a powerful technique used to measure the hydrodynamic size of the colloidal dispersions. The size measurement range of nanoparticles by DLS ranges from 0.6nm to 6 microns. The principle of the measurement is based on the Brownian motion of the colloid or the suspension. When a laser beam is shined through a liquid with suspended particles, the beam scatters off of those particles in all directions, resulting in a scattering-angle-dependent intensity pattern. When the particles are experiencing Brownian motion, the intensity pattern also fluctuates randomly. For the purposes of this experiment, the scattering involved is near the lower threshold of Mie scattering, given that the particle sizes are on the order of the wavelength of the incident light. As the particles were in motion the scattering intensity will fluctuate. The fluctuations in the scattering of laser light is detected and the translational diffusion constant is determined which directly provide the hydrodynamic size, calculated using the well known Stokes-Einstein relationship. This technique is useful to obtain absolute measurements of several parameters of interest, like molecular weight, radius of gyration, Translational diffusion constant and so on. [http://www.malvern.com/LabEng/technology/dynamic_light_scattering.htm]

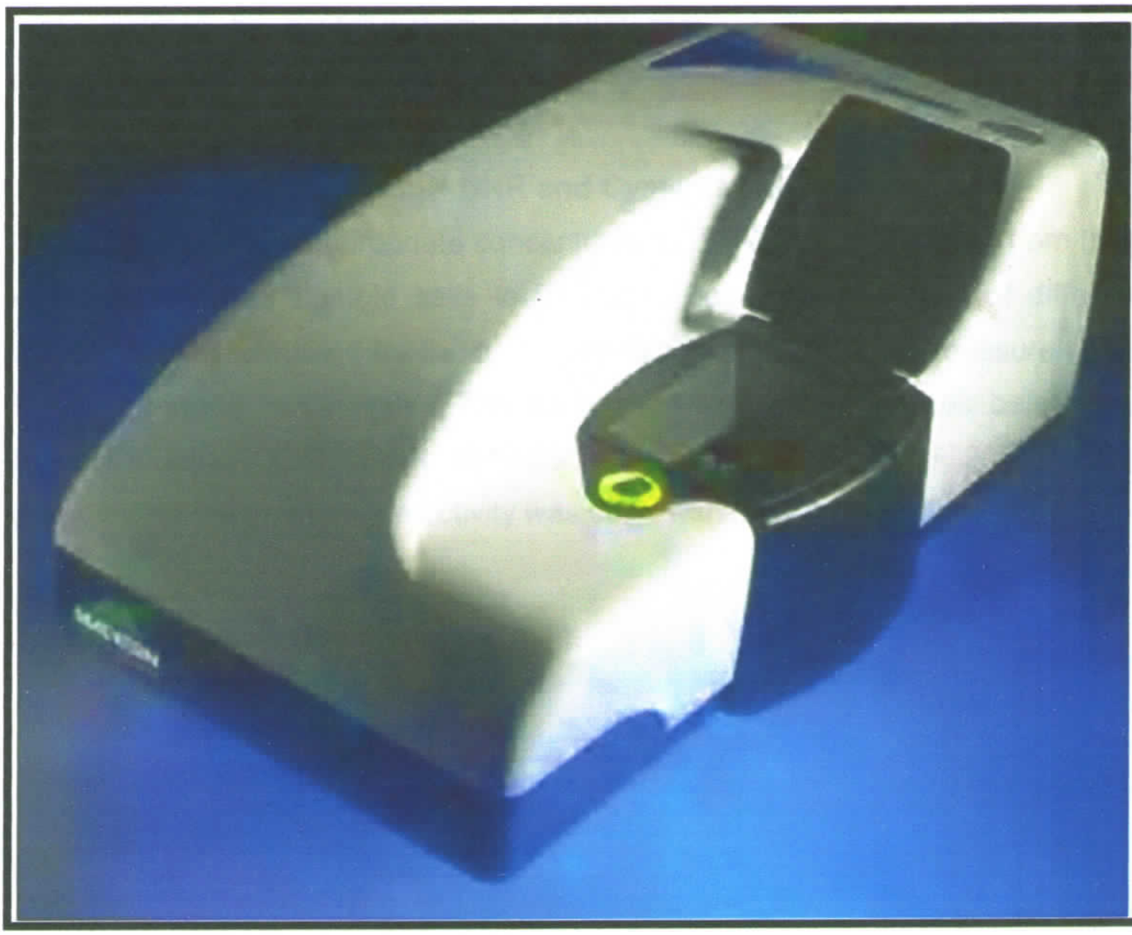

A DLS instrument with multipurpose material analysis. [Malvern Zeta sizer Nano ZS (UK)]

2.2.4 Transmission Electron Microscopy

Electron microscope refers to a family of instruments which produces magnified images by the use of electrostatic or electromagnetic lenses and fast moving electrons. These microscopes have the ability to give images of high or very high resolution over a very useful depth of field.

Simplest electron microscope has two image forming lenses and is an exact analogy of the compound light microscope. The illumination coming from an electron gun is concentrated on the specimen by a condenser lens. After passing through the specimen the electrons are focused by the objective lens into a were isolated by centrifugation at 15000 rpm for 30 minute at 10^{0}C and repeatedly washed with DI water.

2.3.5 Metal Selectivity of GSH GNR and Cysteine GNR using DLS

Metal solutions with appropriate concentrations (1 mM) were prepared from their chloride, nitrate or acetate salts in DI water. Same concentration of different metal ions was prepared for the selectivity test also. All the DLS measurements were performed in DI water. The samples were gently vortexes before the measurements. GSH GNR samples of concentration 0.5mg/ 200µL were prepared for the analysis. Selectivity was done with this concentration.

CHAPTER: 3

RESULTS AND DISCUSSION

CHAPTER 3

RESULTS AND DISCUSSION

The gold nanorods are most attractive nanostructures because of their two SPR bands one at visible (~ 520 nm) and one which is tunable from 600nm to Near Inra Red (NIR). In the reports of Murphy et al. [Sau TK & Murphy CJ.; 2004] the role of size and nature of seed, effect of concentration of seed solution, concentration of AA and concentration of surfactant CTAB were studied in controlling the aspect ratio of gold nanorod. But tuning the aspect ratio with the same concentration of the ingredients has not been discussed. We found that the amount of seed having the same concentration can tune the aspect ratio and SPR of gold nanorods. The similar observation has achieved with AA amount and temperature. Also for the optical sensing applications the short gold nanorods have wide applications as both of its SPR are in the visible region of the electromagnetic spectrum.

3.1 Tuning the AR and SPR with temperature of seed preparation

We prepared the gold seed solution at temperatures 25^{0}C as well as at room temperature (32^{0}C) using 2.2 mM gold chloride, 0.1 M CTAB, 0.01 M sodium borohydride, at 25^{0}C and kept in water bath for 4 hrs after reduction with $NaBH_4$, mainataned at 25^{0}C. Another seed solution was prepared in room temperature using the same concentration of reagents used for the previous experiment. This seed solution was not kept in the water bath.

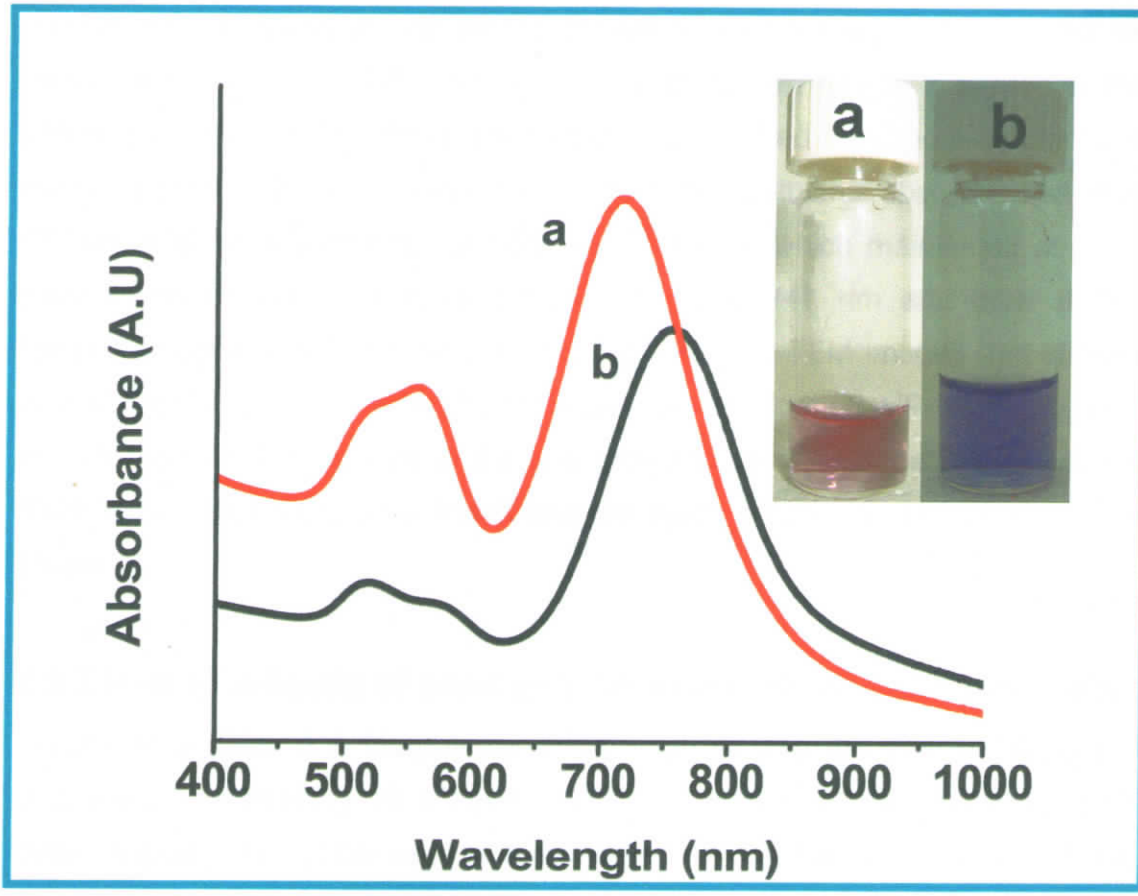

Figure 2 The UV- Visible spectra gold nanorods synthesized using gold seeds grown in different temperatures. Figure 2.a corresponds to the GNR formed by using the seed prepared in room temperature and 2.b corresponds to the GNR formed using seed prepared at 25^{0}C. Inset shows the samples prepared in both conditions.

The gold nanorods were then grown in the same condition at room temperature using the above seeds. Two growth solutions were prepared with 0.01M Silver nitrate, 0.1M Ascorbic acid and 0.1M CTAB. To one of the growth solution 50μL of seed solution from the seed kept in the water bath (25^{0}C, after 4 hour) was added and the other with same amount of seed which were maintained in room temperature. The first growth solution after 30 minutes developed violet to blue color change indicating the rod formation. The second solution (seed at room temperature) didn't show any color in this period but as time proceeds, a pink coloration was developed. After 12 hrs of growth, though the first solution showed a dark blue color, the second growth solution appeared pink in color as shown in Fig 2. The LSPR measurements as shown in Fig 2 inference the difference in the aspect ratio of the gold nanorod formed. The room temperature prepared seed end in lower aspect ratio rod with longitudinal absorption band at 718 nm and transverse band at 556 nm. The seed which maintained at 25^0C gave a red shifted longitudinal plasmon band at 747 nm and blue shifted transverse band at 519 nm compared to the first. The TEM images (not shown) also showed that the short length gold nanorods are formed with seed grown at room temperature compared to the one grown at 25^0C. But the breadth of the GNR in the two experiments hasn't showed much difference in dimension or in shape.

3.2 Effect of amount of seed and AA in the AR of gold nanorods

Murphy et al [Gole A & Murphy CJ; 2004] have studied the size and shape of gold seeds in controlling the AR of the GNR. They observed that along with rods other shaped nanocrystals were also formed on varying the seed size and shape. They also reported the significance of the surface charge of seeds in regulating the size of the rods. In another report [Sau TK& Murphy CJ; 2004.] increase in the AA concentration was found to decreases the rod length.

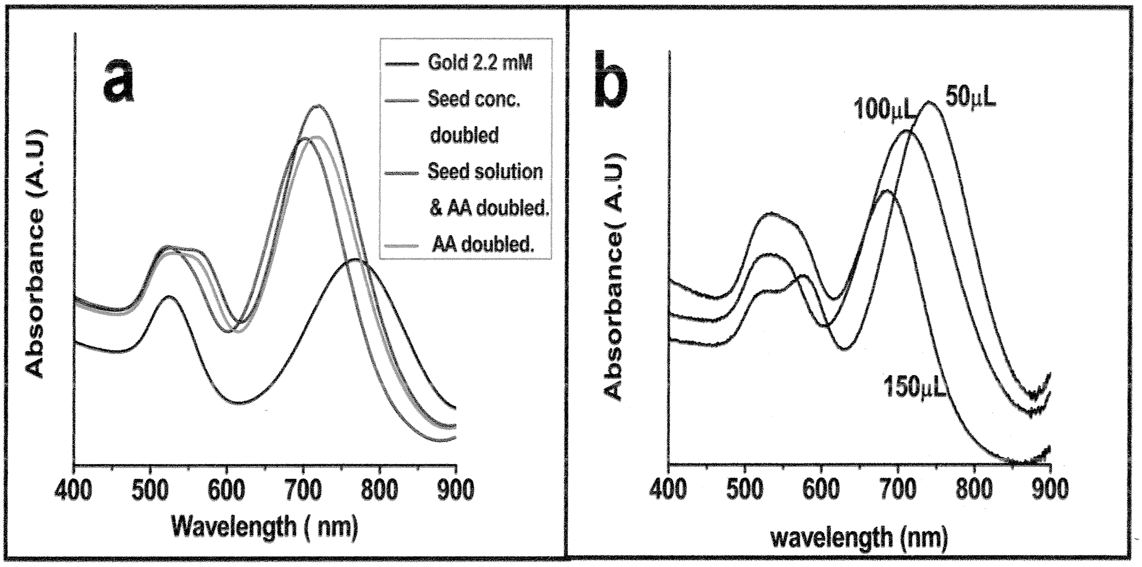

Figure 3 The effect of amount of gold seed and the amount of reducing agent, AA in tuning the optical property of the GNR. Figure 3.a corresponds to the effect of AA in comparison with amount of the seed used. Figure 3.b shows the effect of amount of seed in tuning the SPR property.

Fig 3 shows the SPR of gold nanorods obtained by a serial variation in the amount of the AA and seed. The optimized experiments to synthesis gold nanorod can be seen in the experimental section. When 2.2 mM gold was employed, the GNR formed showed a transverse band at 520 nm and longitudinal at 767 nm (Fig 3.a). As based on the SPR in Fig 3.b, the amount of seed added during the growth of the solution has significant effect in AR and SPR of the GNR synthesized. On increasing the amount of the seeds during the growth of rod the shorter gold nanorods were resulted. On the other hand, when a higher amount (150μL of the seed solution) was used cubical structures along with short GNRs were also formed. This behavior is in agreement with the hypothesis of Murphy et al [Sau TK& Murphy CJ; 2004] that the shorter gold nanorods are the results of the non availability of plenty of Au^{3+} per seed particle. We found that with the supply of the AA to the growth solution, the length of gold nanorod decreased followed by an increase in the yield (yield and AR averaged by counting ~ 30-50 numbers of gold nanorods in the HRTEM image) and hence

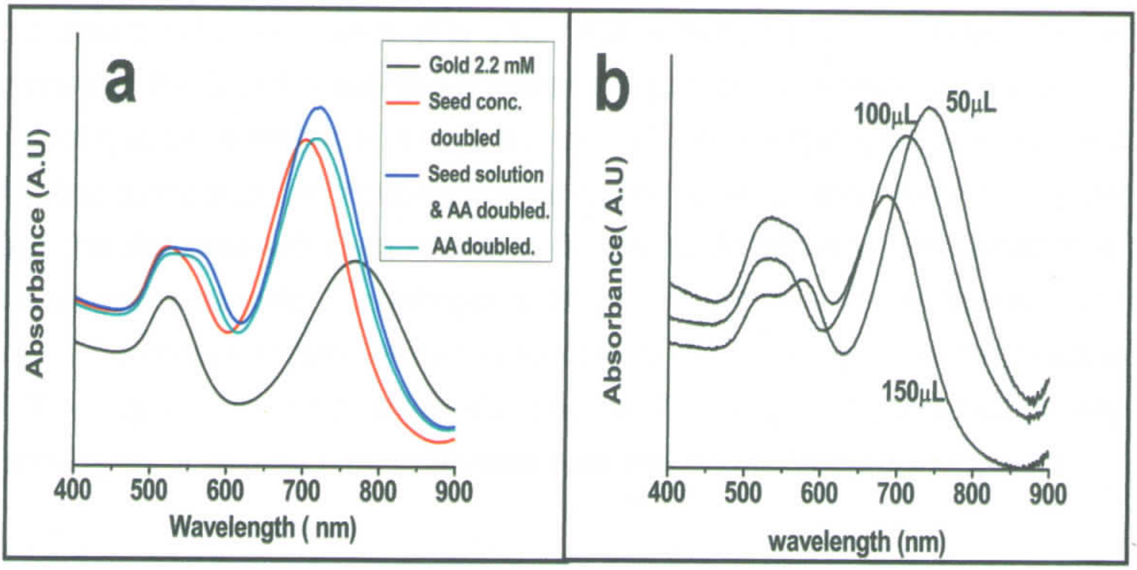

Figure 3 The effect of amount of gold seed and the amount of reducing agent, AA in tuning the optical property of the GNR. Figure 3.a corresponds to the effect of AA in comparison with amount of the seed used. Figure 3.b shows the effect of amount of seed in tuning the SPR property.

Fig 3 shows the SPR of gold nanorods obtained by a serial variation in the amount of the AA and seed. The optimized experiments to synthesis gold nanorod can be seen in the experimental section. When 2.2 mM gold was employed, the GNR formed showed a transverse band at 520 nm and longitudinal at 767 nm (Fig 3.a). As based on the SPR in Fig 3.b, the amount of seed added during the growth of the solution has significant effect in AR and SPR of the GNR synthesized. On increasing the amount of the seeds during the growth of rod the shorter gold nanorods were resulted. On the other hand, when a higher amount (150µL of the seed solution) was used cubical structures along with short GNRs were also formed. This behavior is in agreement with the hypothesis of Murphy et al [Sau TK& Murphy CJ; 2004] that the shorter gold nanorods are the results of the non availability of plenty of Au^{3+} per seed particle. We found that with the supply of the AA to the growth solution, the length of gold nanorod decreased followed by an increase in the yield (yield and AR averaged by counting ~ 30-50 numbers of gold nanorods in the HRTEM image) and hence the aspect ratio also varied (Fig 3.a). We reasoned that an increase in the amount of the reducing agents will create a large number of nuclei for the growth resulting in the formation of a large number of smaller length gold nanorods. But the low quantity of the reducing agents create lesser number nuclei for growth and the Au^0 units will keep on added to this nuclei effecting the formation of larger gold nanorods. Interestingly in all experiments the monodispersity was high. The transverse band of the rod was at 529 nm and longitudinal band was at 716 nm up on supplying double the amount of the AA. We got approximately same types of gold nanorod when both seed and AA doubled simultaneously.

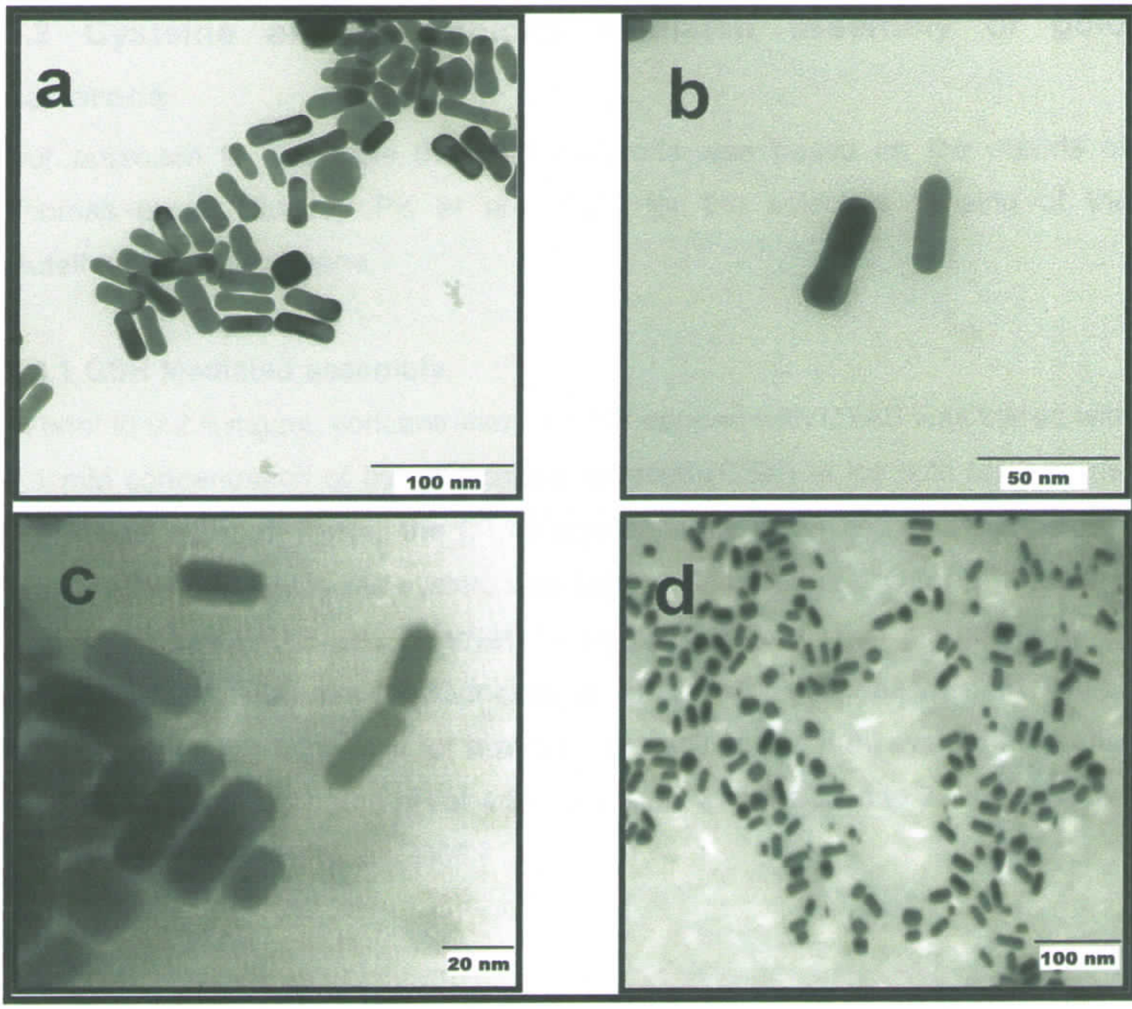

Figure 4 The HRTEM micrographs of the GNR prepared by varying the amount of seed. Figure 4.a and 4.b shows the GNR with AR 3.25, when 50 µL of seed was used. Figures 4.c and 4.d show the GNR with AR 2.36 and 2.33 when seed amount was 100 µL and 150 µL respectively.

The smaller AR gold nanorod was formed when the amount of the seed solution was increased compared to doubling the amount of AA. The AR varied from 3.25, 2.36 and 2.33 as the seed amount increased from 50 µL -150 µL. These studies conclude that instead of making a series of concentration of various reagents, a simple variation of the volumes of the reagents (same concentration) added to the growth solution can be used to tune the features of the gold nanorods.

3.3 Cysteine and Glutathione mediated assembly of gold nanorods

Our approach to assemble the gold nanorods was based on the reports of Thomas et al. [Sudeep PK et al.; 2005] for the selective sensing of the glutathione and L-cysteine.

3.3.1 GSH Mediated assembly

In brief to a 2.5 mg/mL concentration of GNR capped with CTAB was stirred with 0.1 mM concentration of the glutathione reduced (GSH) at ice cold for 3 hours. After three hours of stirring the CTAB was separated from the GNR surface by GSH exchange. Firstly the system was kept undisturbed at 4^0C for 2 hours and the settled free CTAB was removed by simple filtration. Then the solution was centrifuged at 15000 rpm for 30 minute at 10^0C. The pellet was washed with DI water and process continued for two more times. The resultant system here after called as GNR GSH, had a pH of 4.5 and the pH was reduced to 3.5 for effective self assembly. [Sun Z et al.; 2008.]

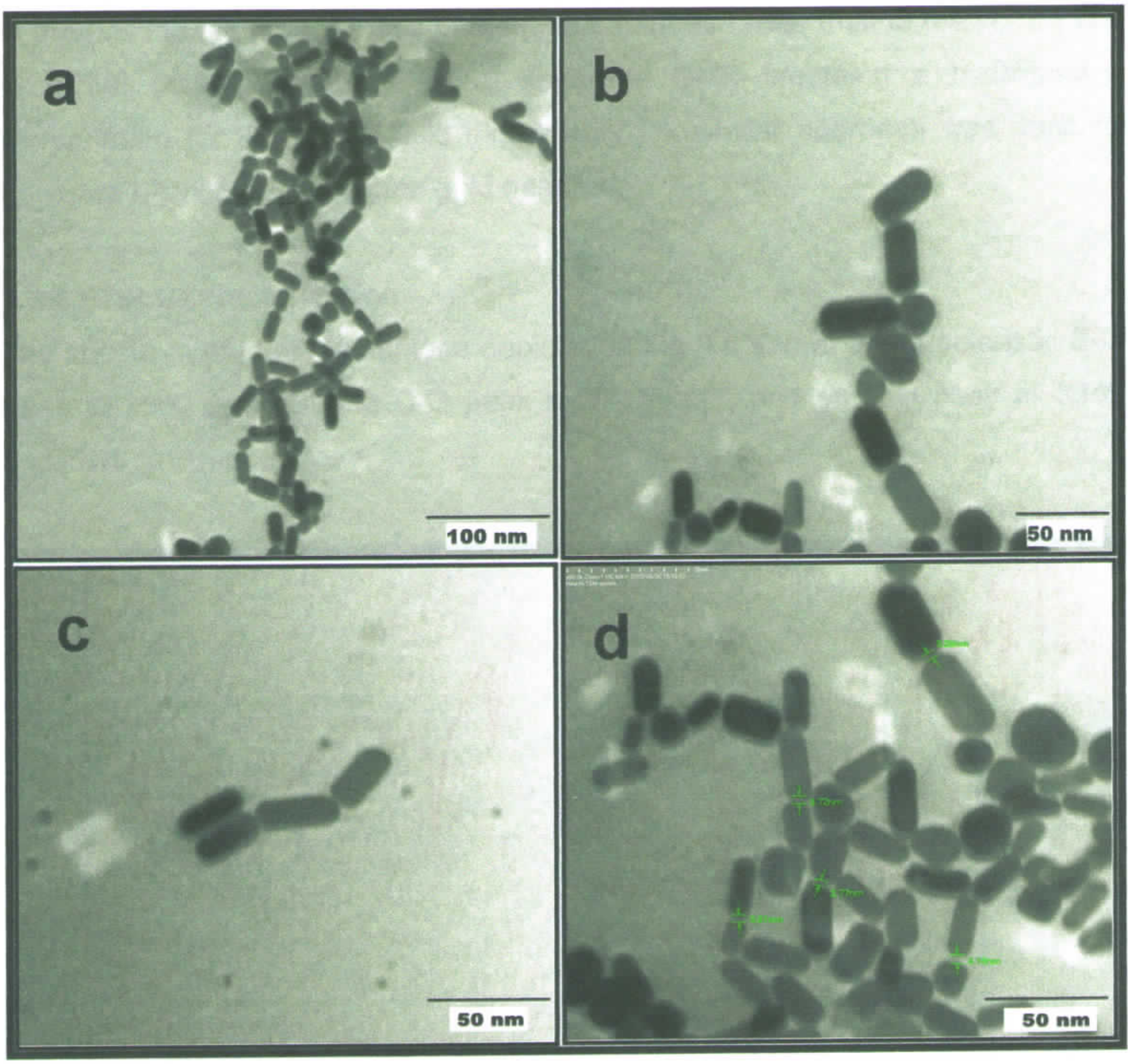

Figure 5 The HRTEM micrograph of the chained GNR using GSH at the end of the GNR. The images a. b. c .d corresponds to the different regions from the copper grid.

The HRTEM images (Fig 5) of the sample showed chain like structures formed through the end to end connection of gold nanorods. The end to end connectivity is supposed to originate through the cooperative intermolecular hydrogen bonding between the molecules of GSH. Figures 5.a, 5.b and 5.c show the images taken from different areas from the copper grid. The average spacing between the rods was found to be 3.49 nm as shown in Fig 5.d. Any side by side alignment was nearly absent as seen in the micrograph. The images clearly indicate the end to end connection was due to the attachment of the thiol group of the GSH to the {1, 1, 1} face of the gold nanorods rather than to the {1, 1, 0} or {1, 0, 0} faces where the CTAB caps the GNR createing a hydrophobic environment for the amino acid dimerization. A similar approach was done to generate L-cysteine connected gold nanorods.

3.3.2 FTIR Characterization

The spectrum of pure Glutathione depicted in Fig 6.a shows a characteristic S-H peak at 2500 cm^{-1}, Strong C-O peak at 1713 cm^{-1}, and an N-H peak at 3346 and1661 cm^{-1} respectively.

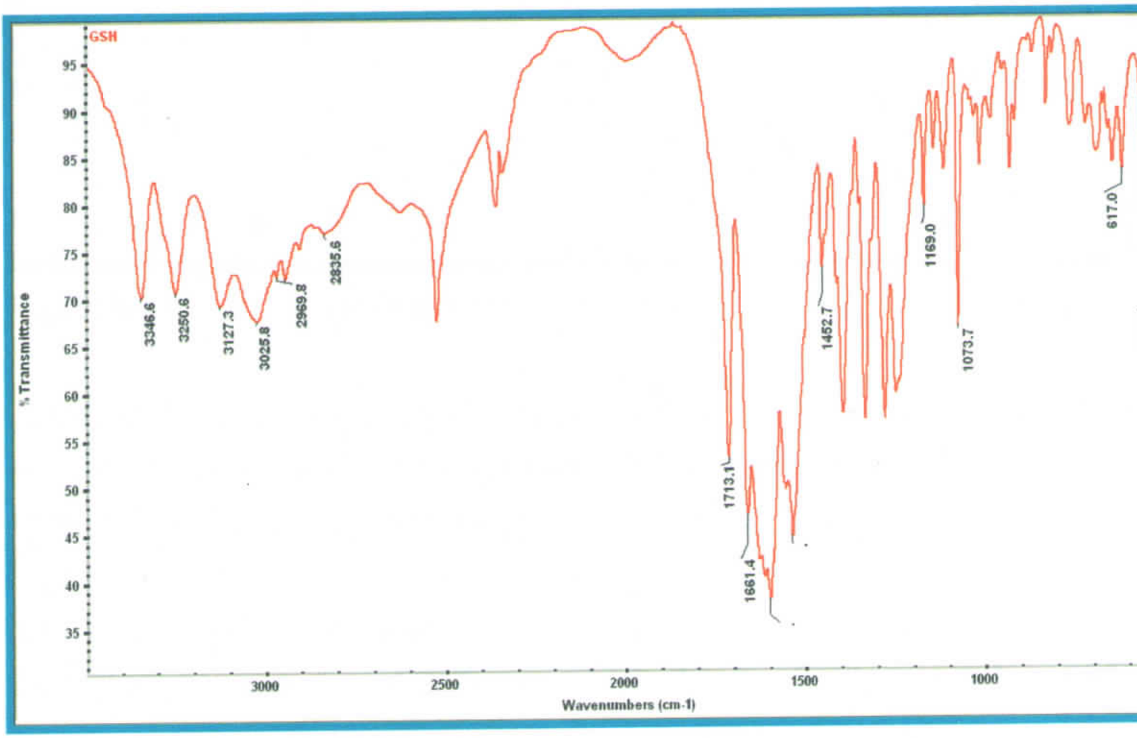

Figure 6.a FTIR spectra of Pure Glutathione reduced.

After functionalizing GSH to CTAB gold nanorod, S-H peak was vanished reflecting the formation of Au-S bond. The FTIR spectrum of GSH coupled GNRs is shown in Fig 6.b.

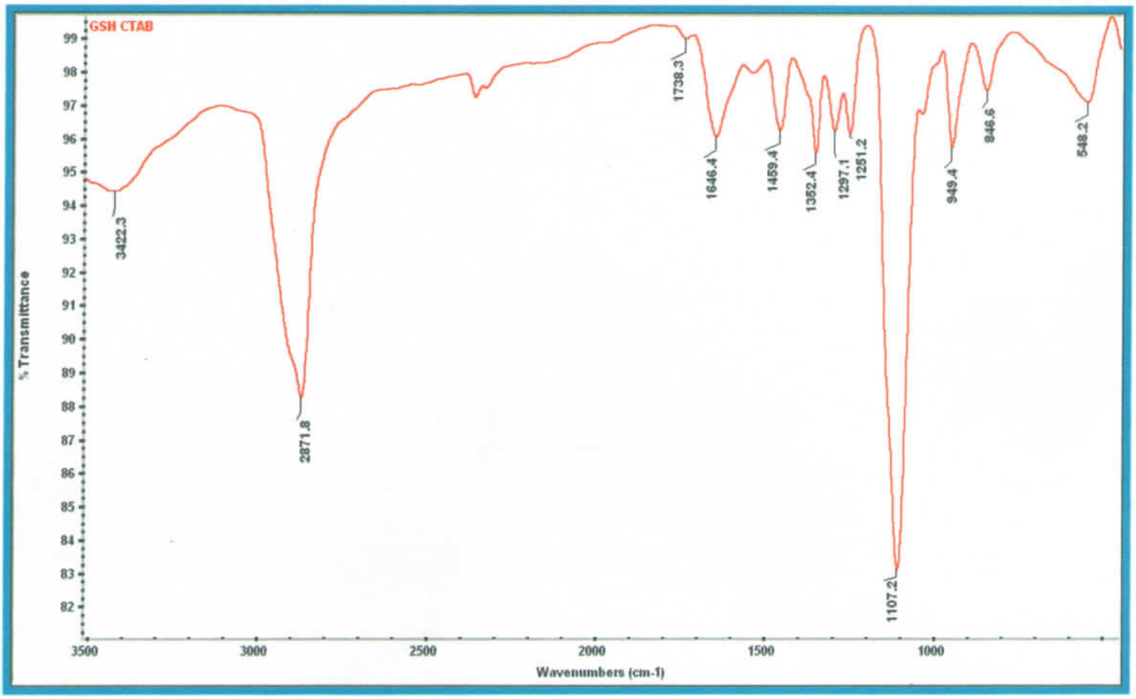

Figure 6.b FTIR spectra of Glutathione functionalized GNR.

Apparently, the spectrum suggests the formation of GSH conjugated GNRs. As a result of the chain like assembly formation, C-O and amide peaks were shifted to 1738 cm^{-1} and 1646 cm^{-1} respectively.

3.3.3 Cysteine Mediated assembly

2.5 mg/ mL concentration of GNR capped with CTAB was stirred with 0.1 mM L-cysteine hydrochloride monohydrate for 3 hours. Excess CTAB was removed by simple filtration and unreacted reagents were washed out by centrifugation at 15000 rpm 30 minute at 10^{0}C. The pellet was redispersed in DI water and the process was repeated twice.

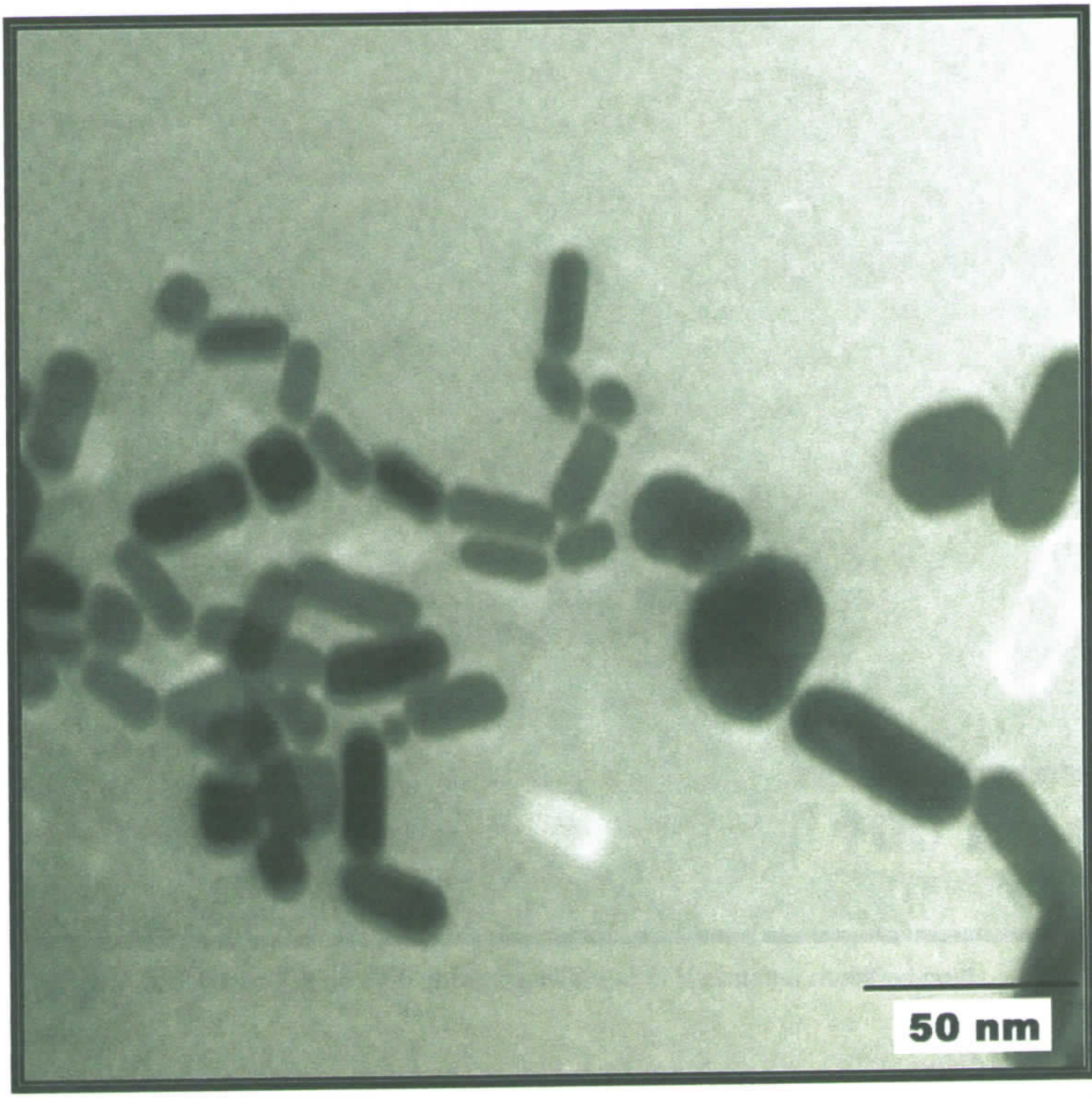

Figure 7.a

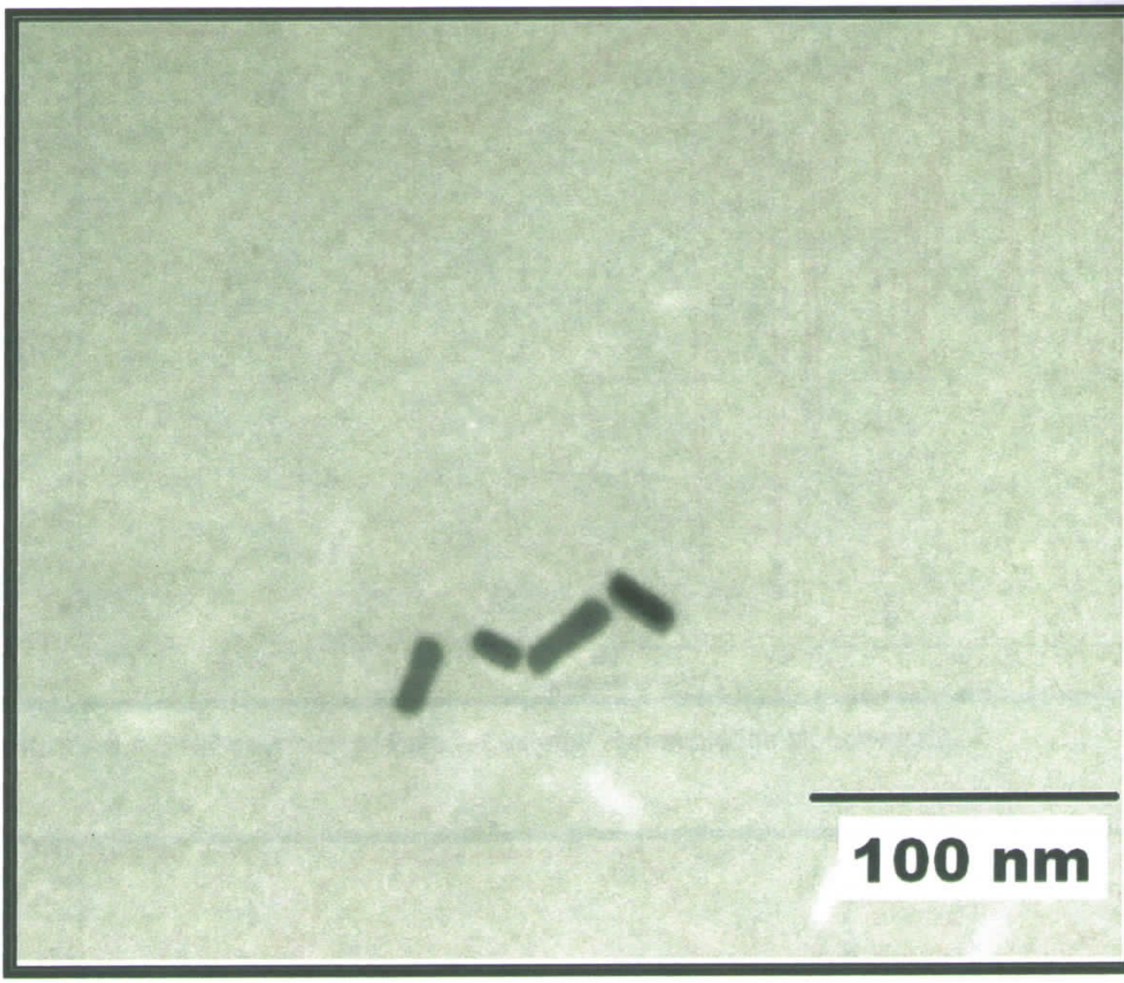

Figure 7.b. Figures 7.a and 7.b show the HRTEM of L-cysteine modified gold nanorods.

3.3.4 FTIR Characterization

Pure L cysteine show characteristic S-H peak at 2563 cm^{-1} , N- H peak at 3368 cm^{-1} and 1620 cm^{-1} , C-O peak at 1736 cm^{-1} (Fig. 8.a).

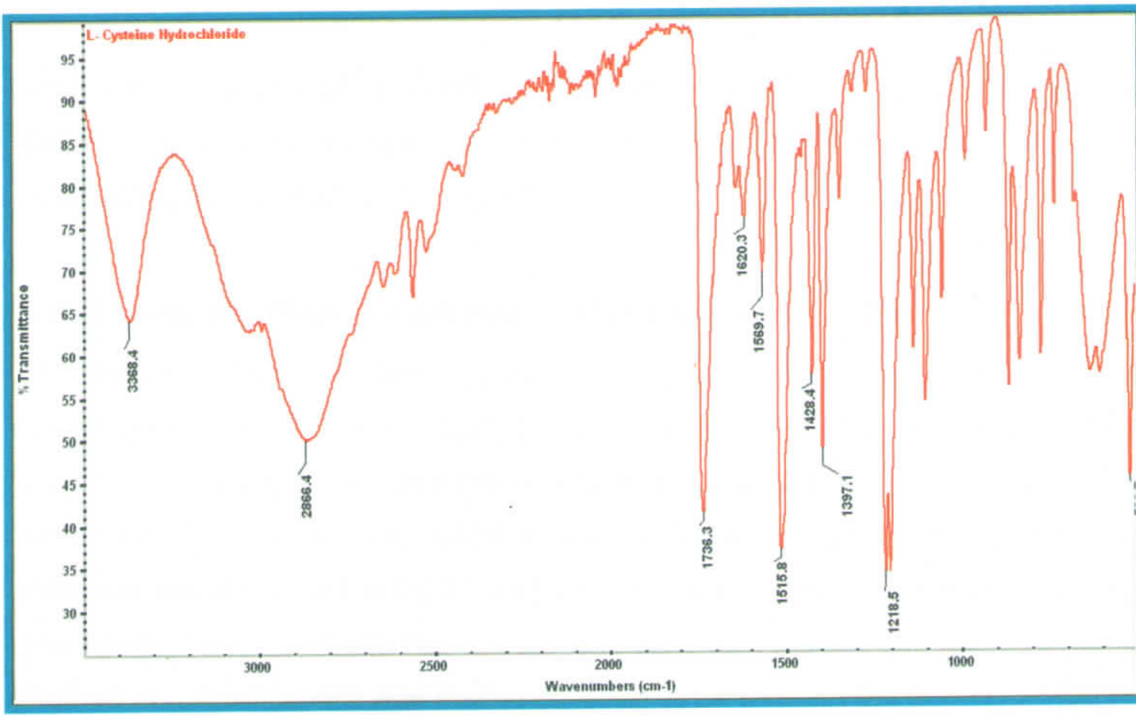

Figure 8.a FTIR spectrum of Pure L-Cysteine Hydrochloride Monohydrate.

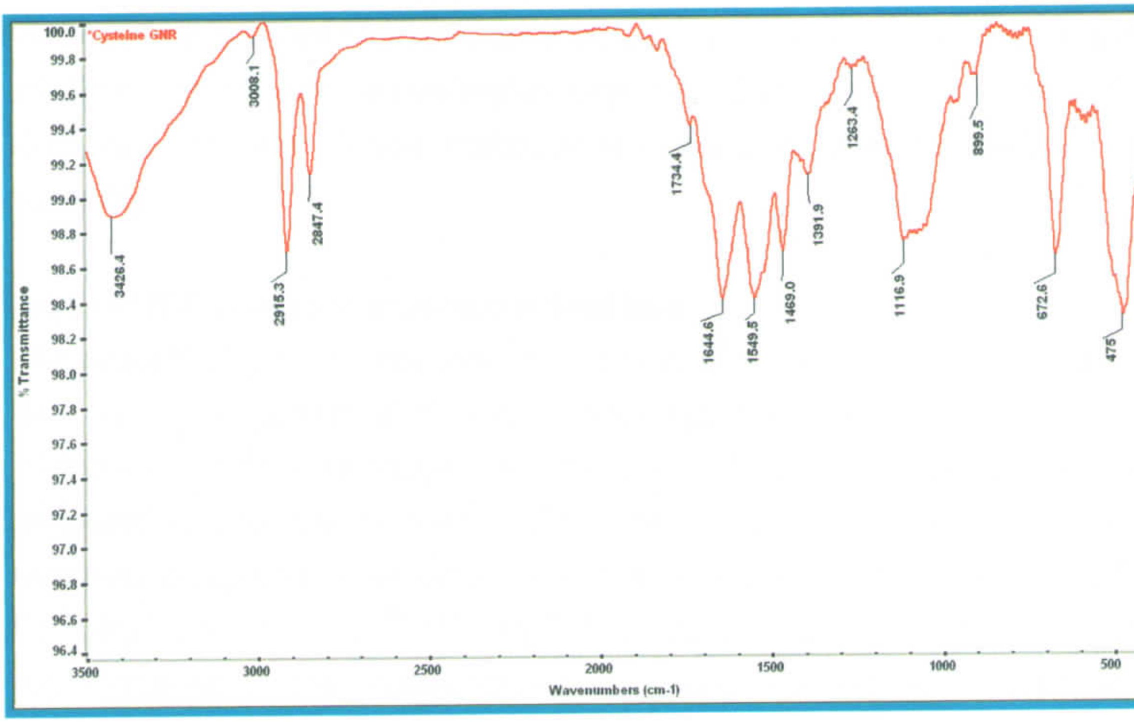

Figure 8.b FTIR spectra of L-Cysteine functionalized GNRs.

After functionalizing CTAB GNR with L-Cysteine, 2563 cm^{-1} peak was missed due to gold sulpher bonding. C-O peak was observed at 1734 cm^{-1} while N-H peak appeared at 3426 cm^{-1}. (Fig.8.b)

3.4 Disassembling the chained GNRs with metal ion

The affinity of the GSH and Cysteine towards the heavy metal ions is a well known phenomenon. Many studies [Wu G et al.; 2004, Franco R et al.; 2007, Ueno Y et al.; 2002.] show that the GSH has an important role as an endogenous antioxidant to increase the cellular viability by scavenging the free radicals (reactive oxygen species-ROS) and also to reduce the carcinogenic effects. Transport of heavy metals like copper and selenium across cell membranes (a method of detoxification) was mainly believed to be through the GSH complexes. Among the amino acids GSH contains six potential coordination sites for the metal binding. Ballatori et al [Ballatory N; 1994.] reported the significance of GSH in controlling the homeostasis in body. Among the various functional groups of the GSH, the sulfhydryl shows highest affinity towards the metal ions like Cu^{2+}, Cd^{2+}, Hg^{2+}, Pb^{2+} etc. These studies, in fact, prompted us to test the nanorod assembly with metal ions.

3.4.1 HRTEM studies in presence of lead ions

The assembled gold nanorod (see fig 5) was viewed using HRTEM after adding different concentrations of Pb ions. Interestingly the chained gold nanorods (GSH) were found to be broken down by the presence of Pb. This disassembly motivated us to explore the system for selective sensing of the cation, Pb^{2+}. The selectivity was tested in presence of various other heavy metal ions like Cu^{2+}, Cd^{2+}, Hg^{2+}, Zn^{2+}, Mn^{2+}, Co^{2+}, Ni^{2+}, Mg^{2+}, $NH_4{}^{+}$etc. Except Hg^{2+} all other analytes didn't respond to the disassembly. But a higher concentration of mercury interfere the analysis.

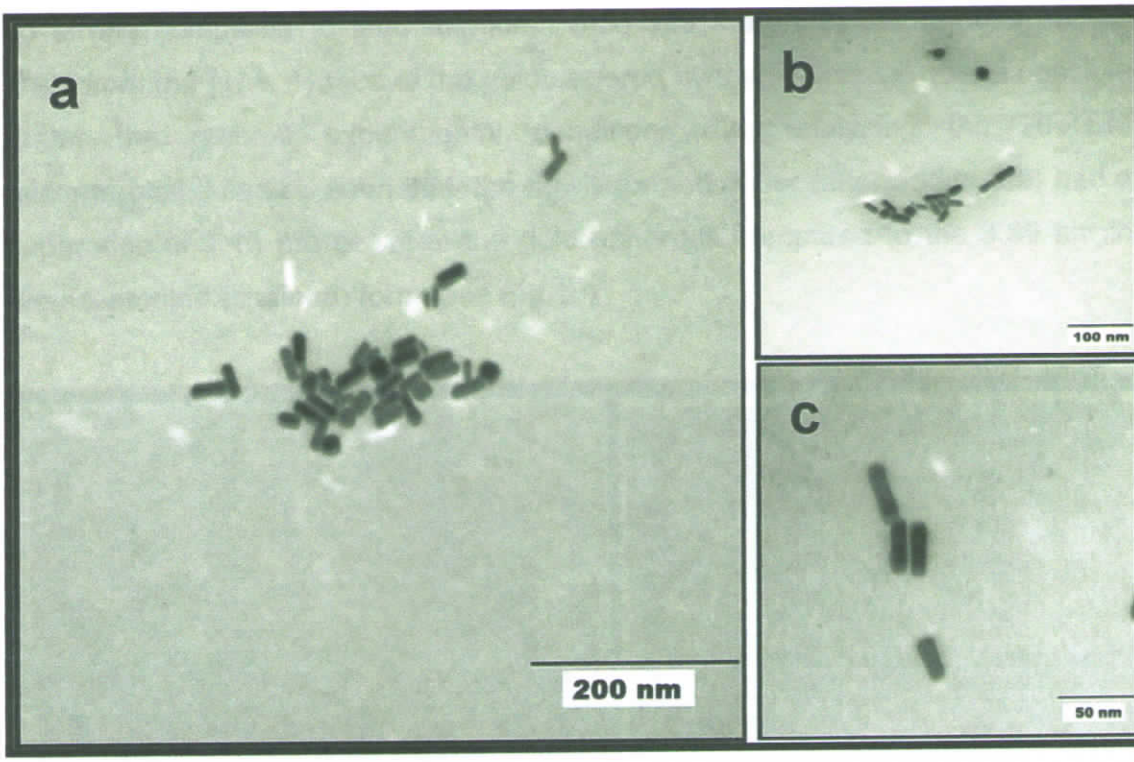

Figure 9 The HRTEM micrographs show the disassembly of aggregated GNR by Pb ions. The chained rods were broken and selectively dimmers were seen in different regions in the sample dropped on the copper grid (a, b and c).

Fig 9 shows the disassembled gold nanorods. The chained nanorods were broken and a number of dimer of GNR was observed in the HRTEM micrographs. The dimers are hypothesized due to the complex formation of the broken chain with the Pb^{2+} through the carboxyl and amine groups. This is against the reports of the previous study of Ali et al. on quantum dots [Ali EM et al.; 2007.]. Their study pointed out that Pb selectivity was completely due the interaction with the –SH part of GSH which will ultimately results in the fluorescence quenching of the quantum dots due to surface un protection. The gold – sulphur (Au- S) interaction and the strength and properties of the gold nanomaterials up on thiolation process have been subjected to extensive studies [Love JC et al.; 2005, Cossaro A et al.; 2008, Gronbeck H et al.; 2000, Grandbois M et al.; 1999, Bourg MC et al.; 2000.]. The studies show that the {1, 1, 1} face of gold has high affinity towards the sulphur. So we believe that the Au-S bond is so strong compared to lead-sulphur (Pb-S) and therefore, the removal of the GSH from the {1, 1, 1} face of the gold nanorod by the Pb ion will not be possible under the present experimental conditions. On analyzing the HRTEM micrographs, it can be seen that, the newly formed dimer (after adding Pb) had a separation of 7.13 nm between the gold nanorods compared to the 3.39 nm in the assembled (chained) form (see Fig 10)

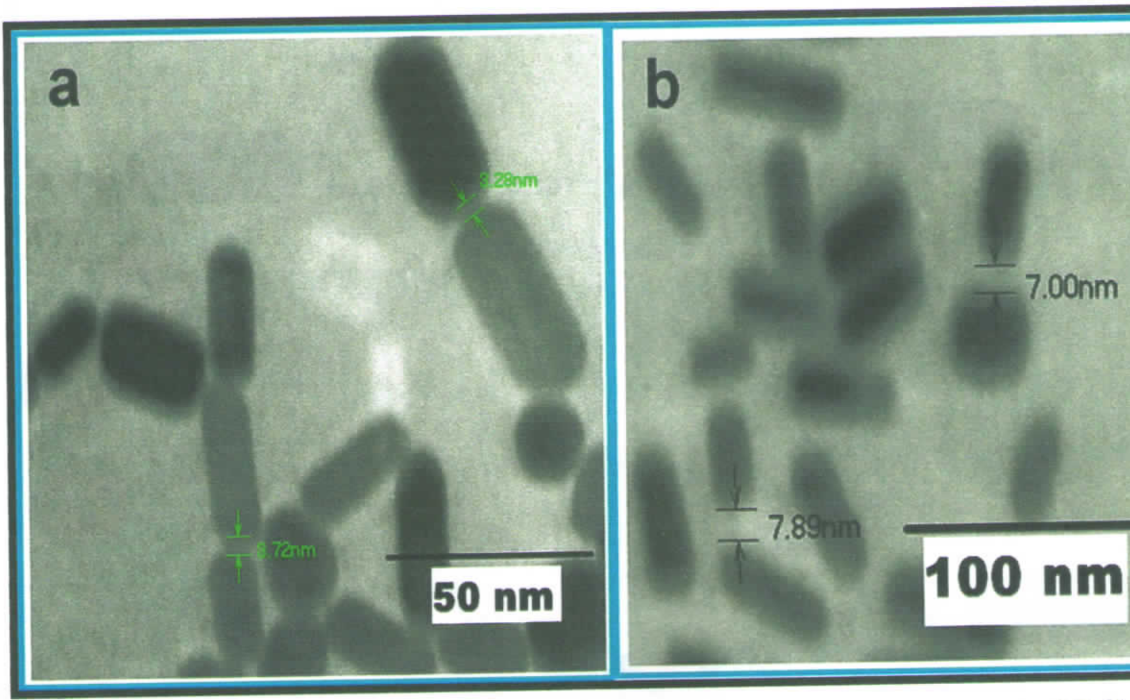

Figure 10 The assembled (GSH modified) GNR (a) and GSH GNR in presence of Pb^{2+} (b)

This clearly supports our view that the Pb ion is selectively complexes with the glutamyl carboxyl and glutamyl amino groups. Such a mechanism may lead to dimer with separation due the Pb atoms. But at the same time the aggregation o chained gold nanorods at some regions may be the result of the comple formation with sulfhydryl residue in GSH as per the report of Ali et al. [Ali EM e al.; 2007]. However, in the aggregated structures as seen in the HRTEM dimmers are dominated. Our view also supported by the reports of Bala et al. [Bala T et al.; 2007] that the carboxylic acid group has affinity towards the divalent metal ions. Their study shows that among the heavy metal ions the pb^{2+} has more affinity to bind with the carboxyl residue compared to Cd^{2+}. Based on the HRTEM micrographs we propose the following mechanism (**scheme 4.a & 4.b**) for assembly, disassembly and dimer formation process in gold nanorod for the present study.

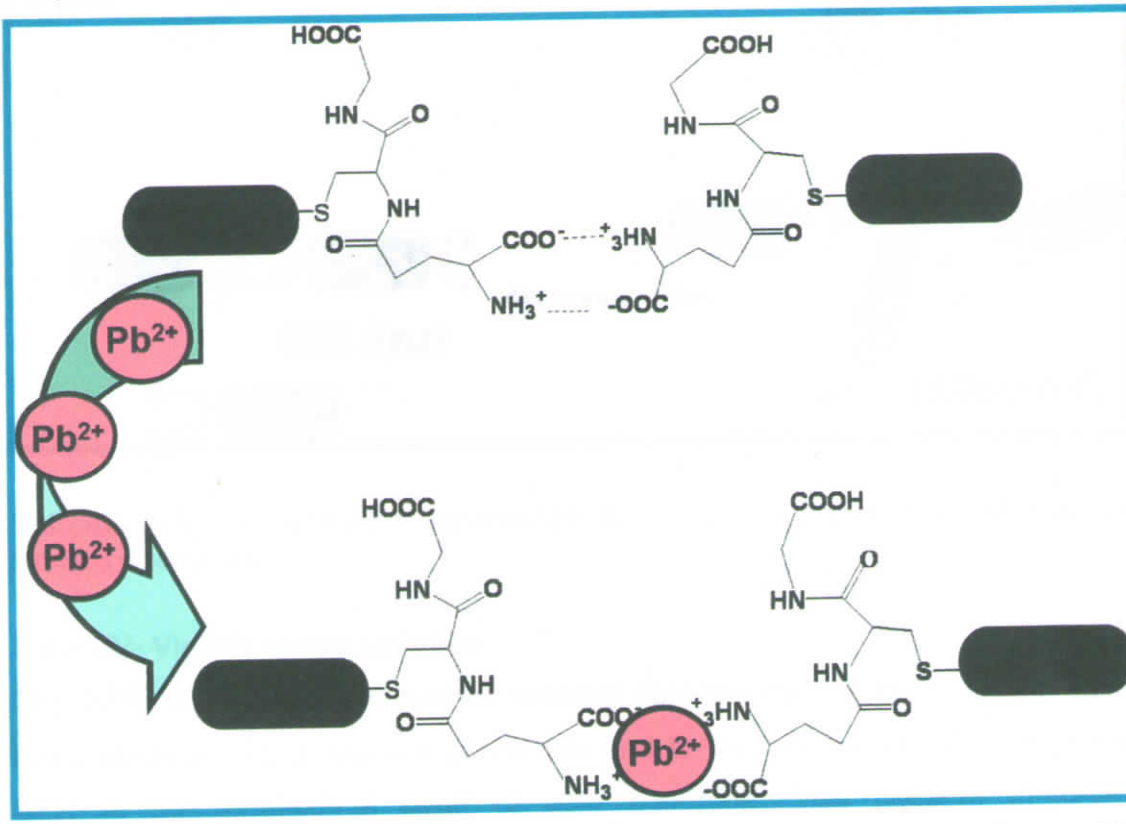

Scheme 4.a The tentative mechanism of gold nanorod assembly and disassembly leading to dimer structure .

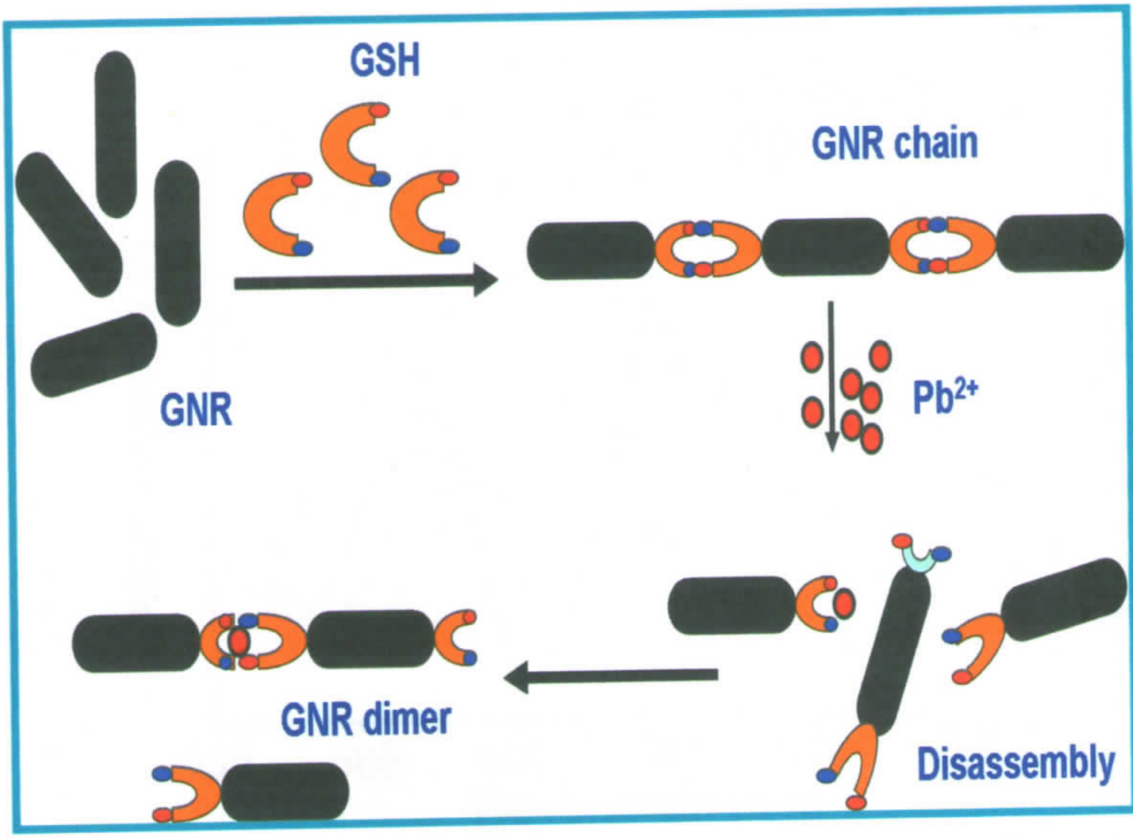

Scheme 4.b The schematic representations of the GNR assembly and lead ior induced disassembly.

3.4.2 UV- Visible characteristics

The SPR is an important tool in sensing applications based on noble meta nanostructures. As discussed earlier the end to end alignment will change the SPR at the longitudinal band of gold nanorods. This became importan characteristics which will confirm the end to end assembly in many studie [Caswell KK et al.; 2003, Thomas KG et al.; 2004, Gole A & Murphy CJ; 2005 Sudeep PK et al.; 2005, Fava D et al.; 2008.]. The gold nanorods which w chosen for self assembly were prepared as discussed in the experimenta section. The CTAB capped gold nanorods were cleaned of free CTAB and th optical features were recorded.

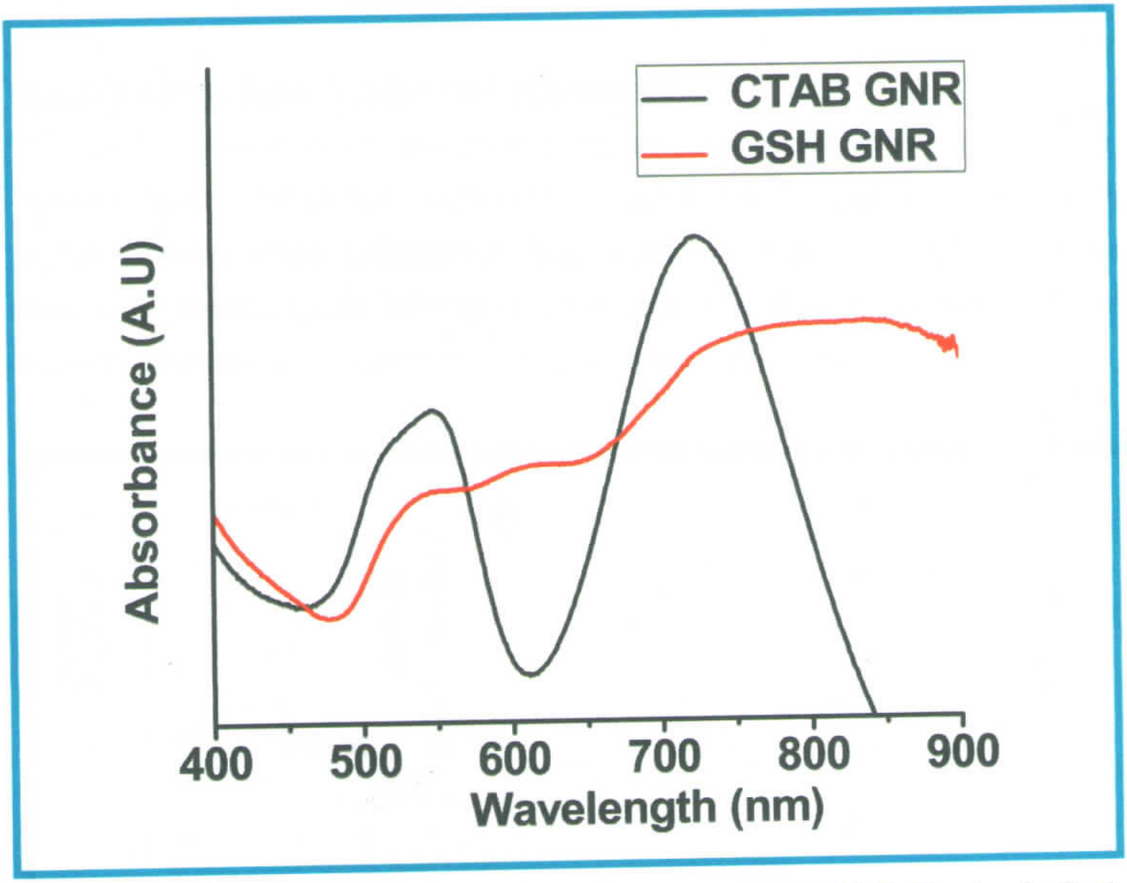

Figure 11 The UV- Visible spectra of the CTAB GNR and GSH GNR. The longitudinal band red shifted to 843nm from the 717 nm.

The CTAB GNR before GSH addition showed the transverse band at 534 nm and longitudinal band at 717 nm (fig 11). After GSH modification the transverse band didn't show any spectral shift but only a reduction in the amplitude. At the same time the longitudinal band red shifted to 843 nm and became broad clearl demonstrating that formation of the end to end assembly. As the aspect ratio o the gold nanorod is small we couldn't make a conclusive evidence of the disassembly in the presence of lead ions. The longitudinal peaks showed 4-6 nm blue shifts in presence of various concentrations of lead ions.

3.4.3 Dynamic Light Scattering Experiments

The DLS measurements with GNR samples gave hydrodynamic size which is greater than the dimensions measured in the HRTEM. This variation may be due to the coverage of the surfactant molecules with water in the measuring medium. The CTAB alone capped GNR gave a hydrodynamic size averaged to 132.51nm from the repeated measurements with good monodispersity.

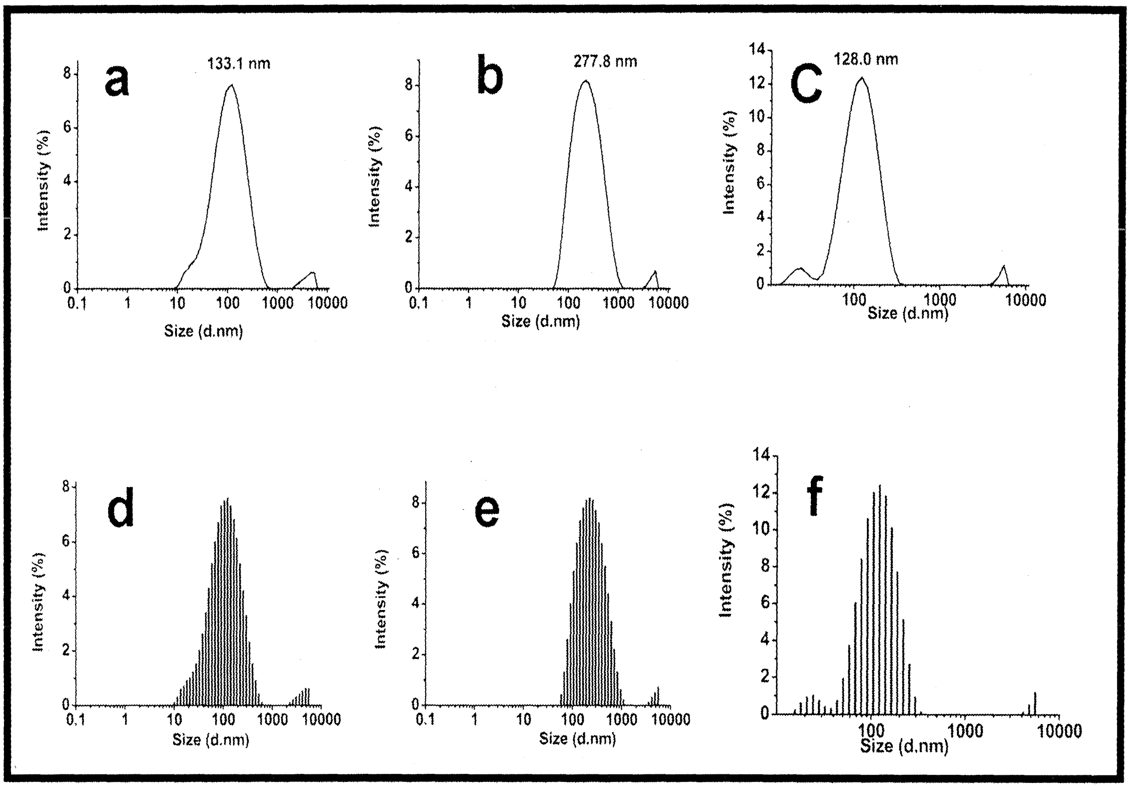

Figure 12 The hydrodynamic size measurements of the CTAB GNR (a), GSH GNR (b) and size of GSH GNR in presence of 0.1mM lead ion. The figures d. e and f correspond to the respective particle size distribution of the samples.

Fig 12.a corresponds to one of such measurement and the size was 133.1 nm. Up on GSH treatment the size changed to 258.83 nm in the initially and later changed to 393.25 nm. One of the measurements (277.8 nm) is shown in Fig 12.b. The increase in the size as the time elapsed indicates the formation of GNR chain. But up on adding 0.1 mM of Pb^{2+} the size changed to 155.55 nm. This inference the GNR chains are breaking and return to the original size, which is in agreement with the HRTEM observation. One of such measurements has shown in fig 12.c. Based on this observation we studied the effect of various concentrations of lead ions on the assembly with a view to generate a concentration – size correlation and thereby to use this novel approach for Pb sensing.

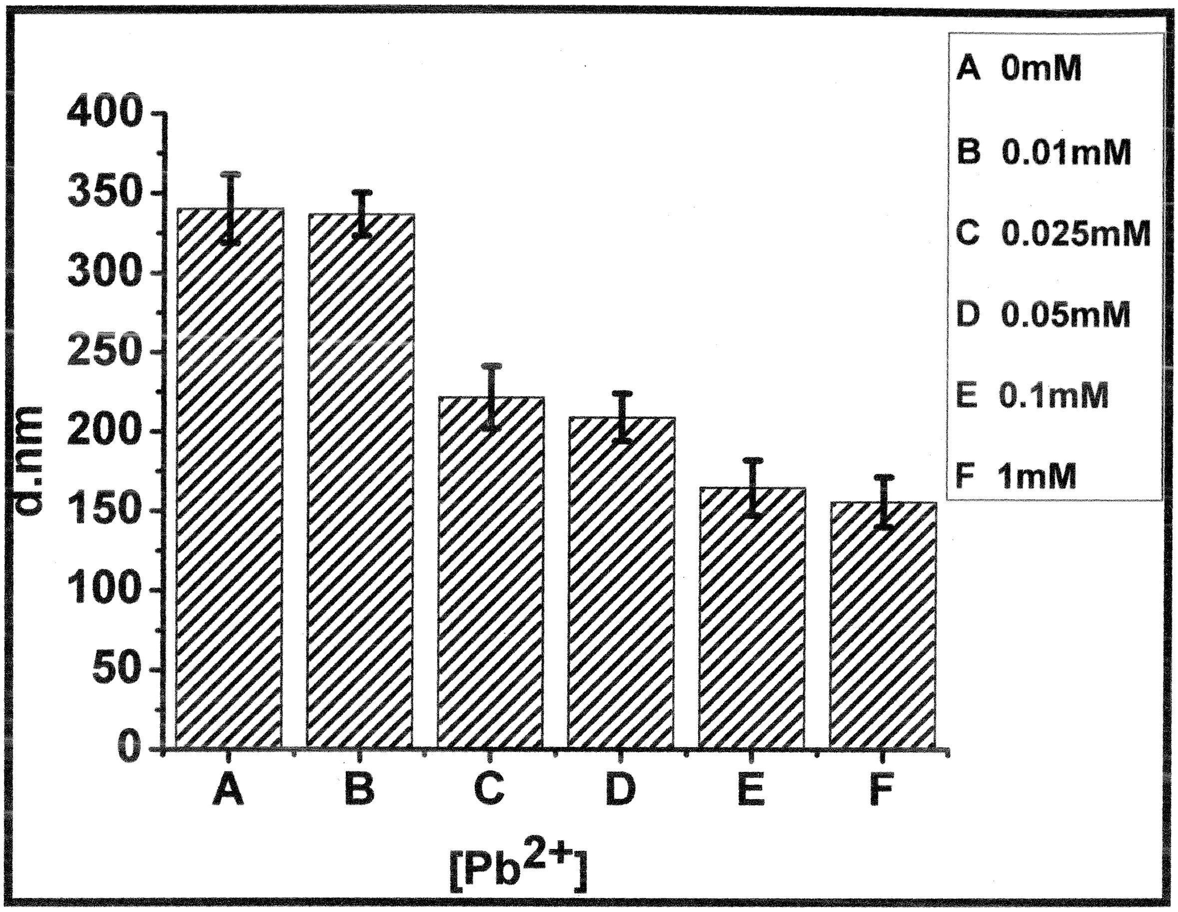

Figure 13 The Limit of detection (LOD) of the lead ion based on the changes in the hydrodynamic size of the GSH GNR. The plot is constructed by plotting the size against the concentration.

Fig 13 shows the effect of concentration of Pb ions on the size of GNR. We could observe a decrease in size between a concentration ranges of 0.1 mM -0.025 mM. Our DLS data indicate that the sizes of the rods were reduced appreciably within a concentration of 0.1 mM -0.025 mM. Below 0.025 mM there was no measurable change in the size of the GSH GNR. In that sense, we came to the conclusion that the Limit of Detection (LOD) of the present system for Pb is 0.025 mM. Our results indicate that analyte induced disassembly of assembled gold nanorods is an interesting approach for the detection and estimation of components of interest.

The selectivity of the system in the presence of other cations was also performed. Metal ions, other than Pb, didn't show detectable response on the nanorod assembly. The response of other metal ions on the hydrodynamic size of the nanorods is shown in Fig 14.

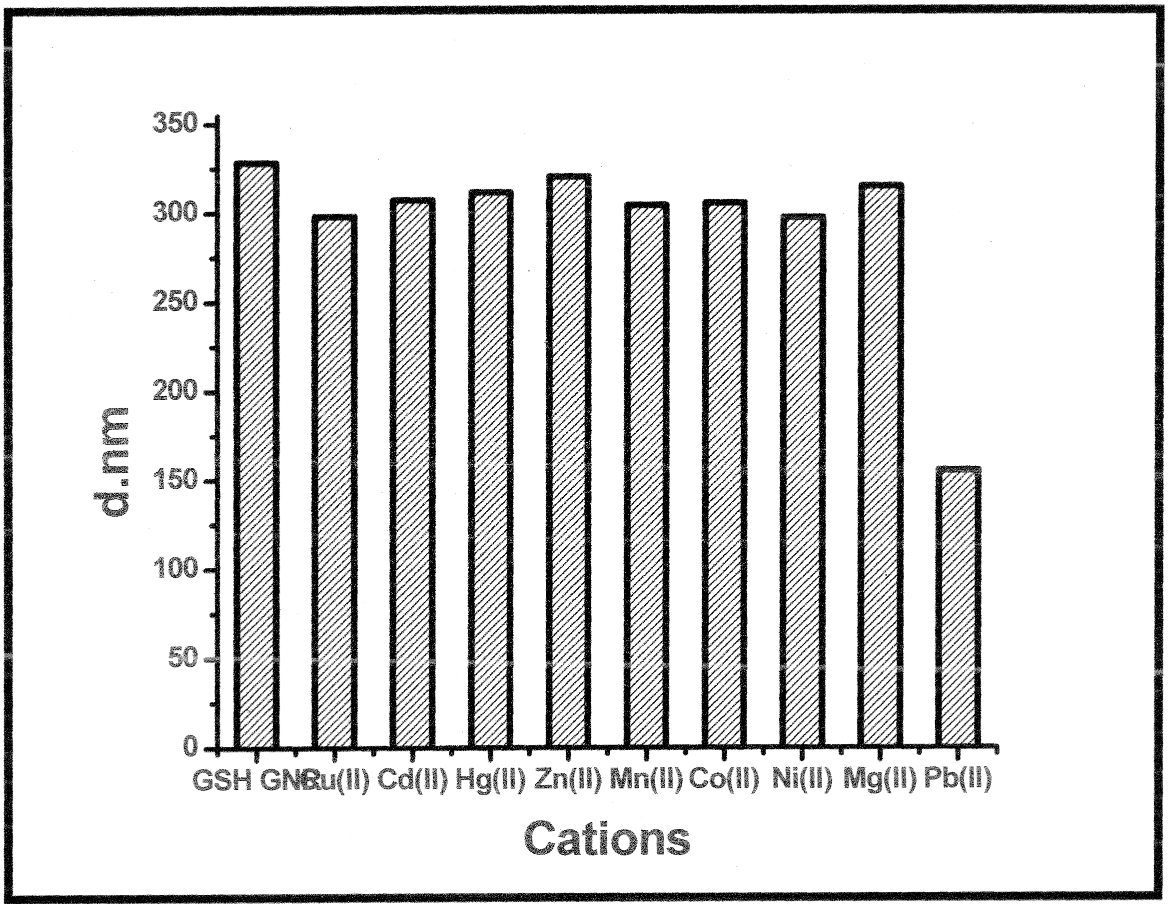

Figure 14 Selectivity of Pb^{2+} over other cations by the GSH modified gold nanorods. The size (d in nm) was plotted against various cations of 1mM concentration.

3.5 Disassembly of Cysteine gold nanorod chain in presence of copper

Cysteine is widely used in many pharmaceutical formulations such as antibiotics and drugs for treating skin damages. It is also a potential neurotoxin, a biomarker for various medical conditions and a physiological regulator. [Li L & Li B; 2009, Wang XF & Cynader MS; 2001, liu J et al.; 2000, Droge W & Holm E; 1997]. Chen et al. introduced a cysteine-modified electrode as a highly sensitive and selective copper (II) sensor, in which a stable five membered ring is formed by the copper (II), the R-amino, and the R-carboxy groups. Proteins containing cysteine, such as metallothionein, will bind metals such as mercury, lead, and cadmium tightly [Baker DH & Czarnecki-Maulden GL; 1987.].These studies show that cysteine can react with heavy metal ions.

3.5.1 UV- Visible characteristics in presence of Copper

The CTAB GNR before cysteine addition showed the transverse band at 539 nm and longitudinal band at 716 nm. After Cysteine modification the transverse band shifted to 519 nm. At the same time the longitudinal band red shifted to 851 nm and broadened.

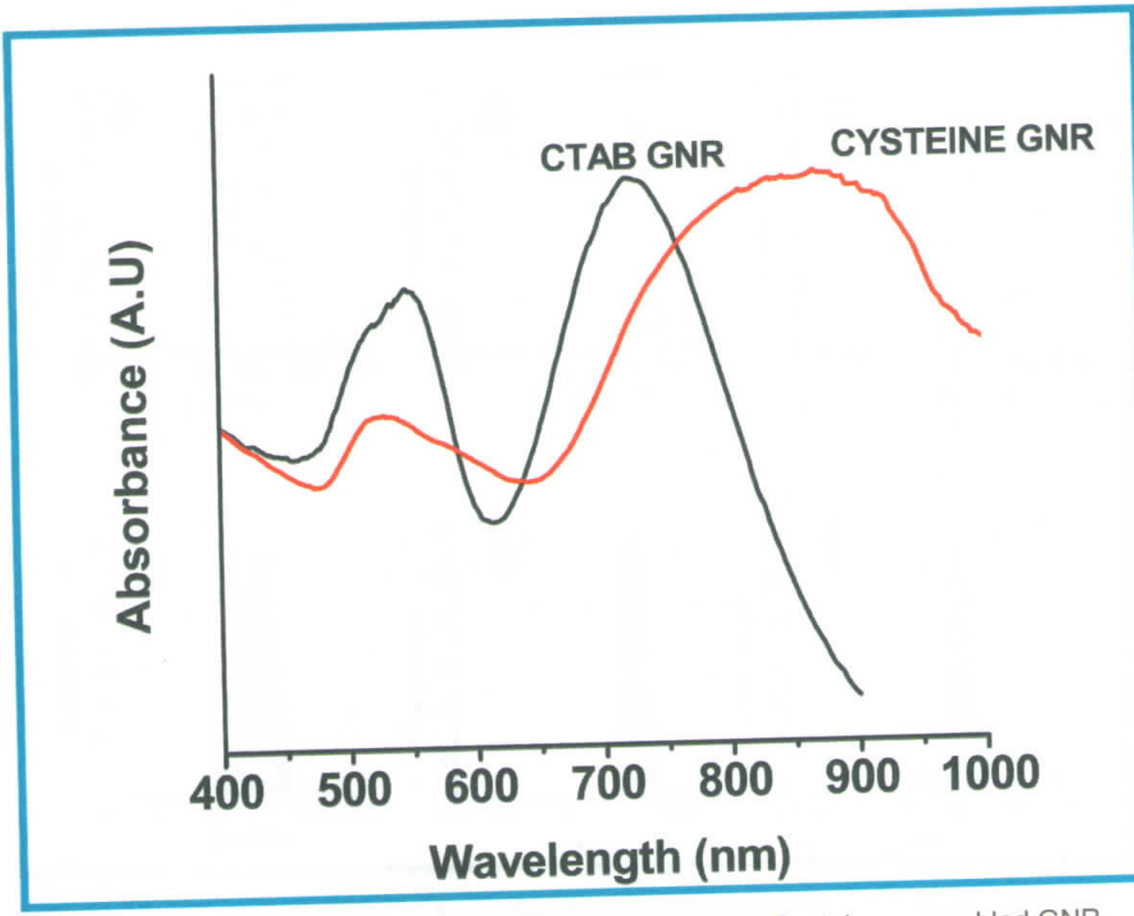

Figure 15 The UV- Visible spectra of the CTAB GNR and Cysteine assembled GNR. The longitudinal band red shifted to 851nm from 716 nm.

The spectrum clearly demonstrates formation of the end to end assembly. As th aspect ratio of the gold nanorod is small we couldn't make a conclusive evidenc of the disassembly in presence of Copper.

3.5.2 Dynamic Light Scattering experiments

The DLS measurements with GNR samples showed a higher hydrodynamic siz than the dimensions measured in the HRTEM. This variation is assigned to th coverage of the surfactant molecules with water in the measuring medium. Th CTAB alone capped GNR gave a hydrodynamic size averaged to 132.51 n from the repeated measurements with good monodispersity.

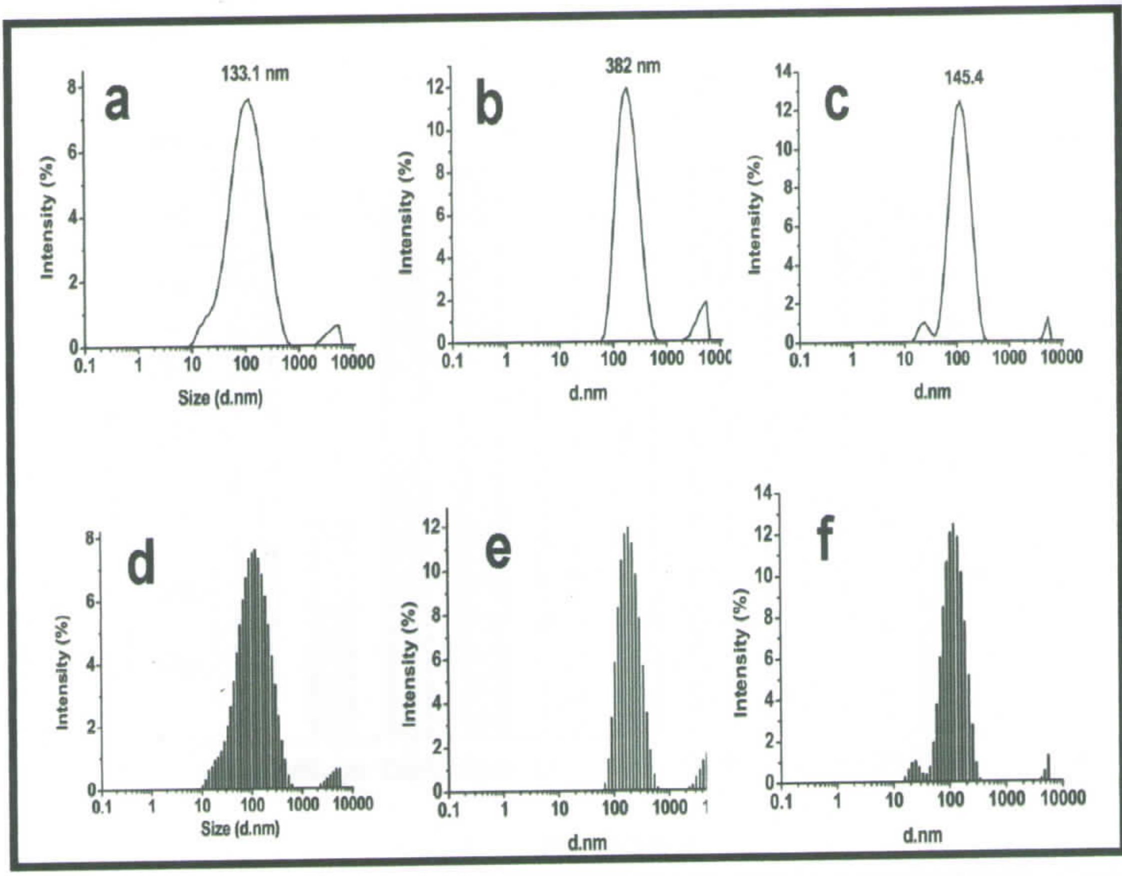

Figure 16 The hydrodynamic size measurements of the CTAB GNR (a), Cysteine GN (b) and size of Cysteine GNR in presence of 0.1 mM Copper ion. The figures d, e and correspond to the particle size distribution of the respective samples.

Fig 16.a corresponds to one of such measurements and the size was 133.1 nm But up on Cysteine treatment the size changed to 382nm, as shown in figur 16.b. The increase in the size as the time progress indicates the formation GNR chain. But up on adding 0.1 mM of Cu^{2+} the size changes to 145.4 n reflecting the breaking of the assembled chains. The size of the particles returned almost to the original size as shown in figure16.c apparently suggestin the disassembly of chain like structure of GNRs by Cu ions.

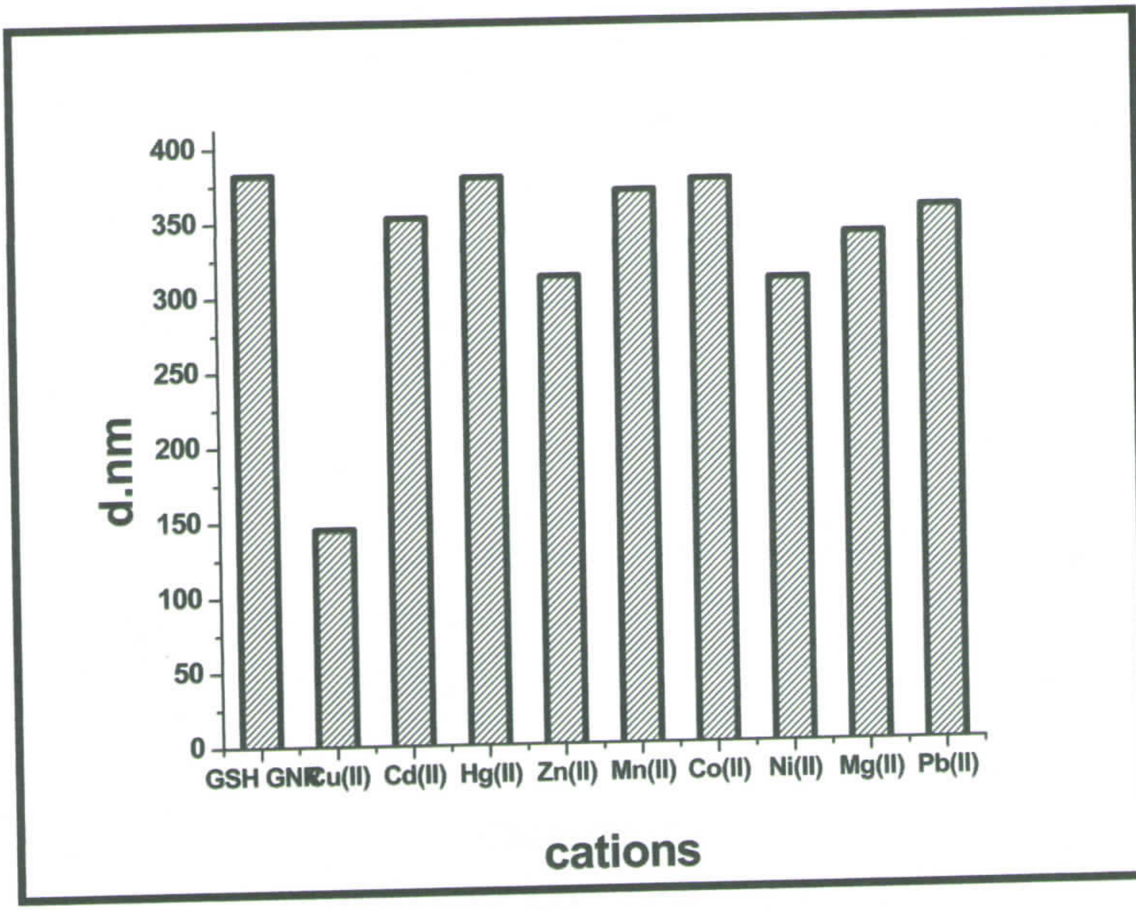

Figure 17 Selectivity of Cu^{2+} over other cations by the Cysteine modified gold nanorods. The size (d in nm) was plotted against various cations of 1 mM concentration.

The selectivity of the system in presence of other cations was also carried out The interferences from other ions were minimal again indicating the feasibility o developing a new copper ion sensor (Figure 17). From the data we could be abl to show that copper can selectively disassemble the cysteine chained GNR. Thi observation can possibly be refined as a new approach for analyzing the Coppe ion concentration.

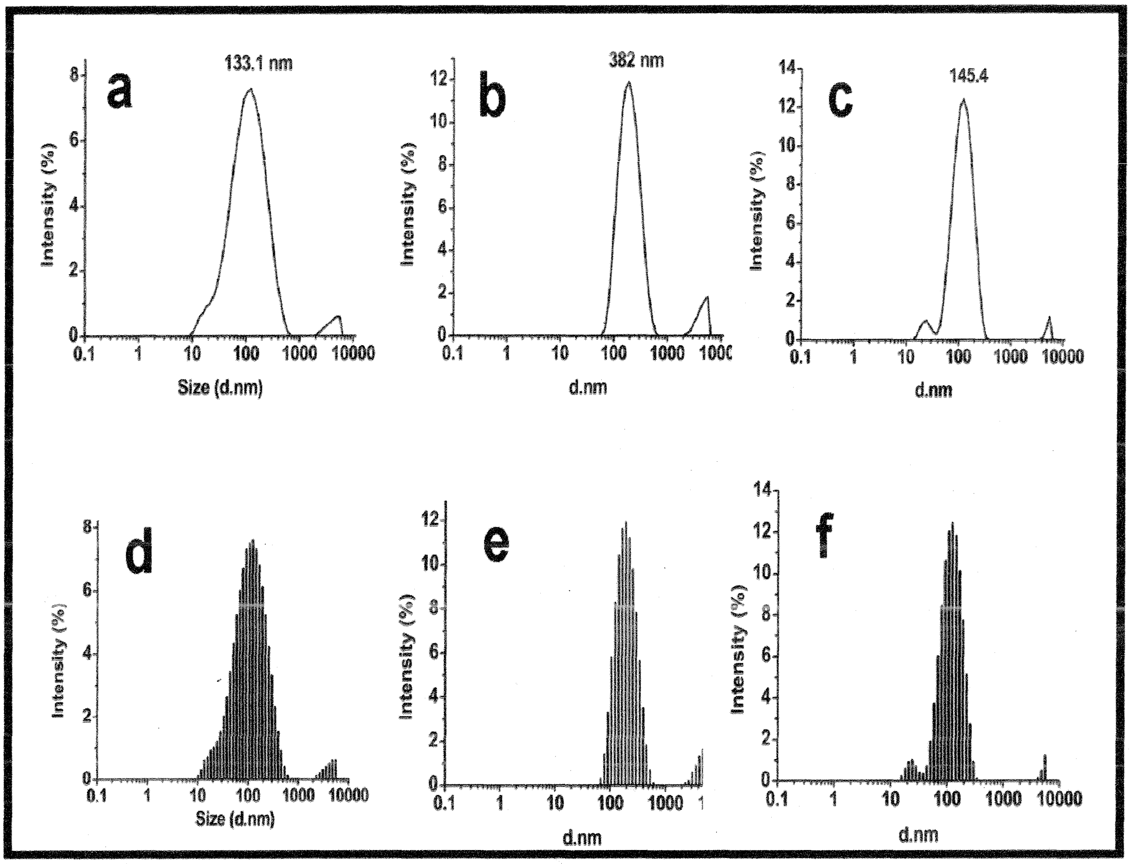

Figure 16 The hydrodynamic size measurements of the CTAB GNR (a), Cysteine GNR (b) and size of Cysteine GNR in presence of 0.1 mM Copper ion. The figures d, e and f correspond to the particle size distribution of the respective samples.

Fig 16.a corresponds to one of such measurements and the size was 133.1 nm. But up on Cysteine treatment the size changed to 382nm, as shown in figure 16.b. The increase in the size as the time progress indicates the formation of GNR chain. But up on adding 0.1 mM of Cu^{2+} the size changes to 145.4 nm reflecting the breaking of the assembled chains. The size of the particles is returned almost to the original size as shown in figure16.c apparently suggesting the disassembly of chain like structure of GNRs by Cu ions.

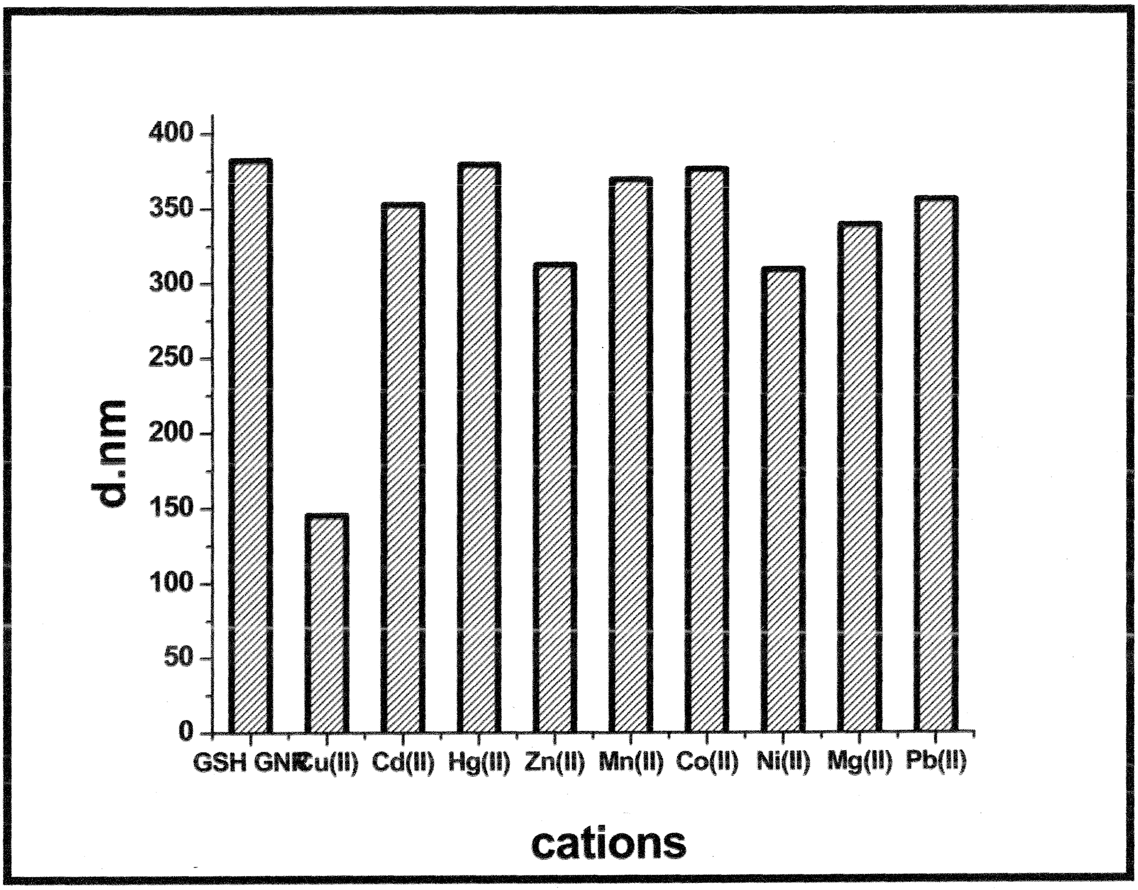

Figure 17 Selectivity of Cu^{2+} over other cations by the Cysteine modified gold nanorods. The size (d in nm) was plotted against various cations of 1 mM concentration.

The selectivity of the system in presence of other cations was also carried out. The interferences from other ions were minimal again indicating the feasibility of developing a new copper ion sensor (Figure 17). From the data we could be able to show that copper can selectively disassemble the cysteine chained GNR. This observation can possibly be refined as a new approach for analyzing the Copper ion concentration.

CHAPTER 4

SUMMARY AND CONCLUSION

CHAPTER 4

SUMMARY AND CONCLUSION

In this work we have shown, for the first time, disassembly of assembled gold nanorods by adding specific heavy metal ions such as Pb and Cu. We explored the nature of glutathione mediated self assembled chains of gold nanorods in the presence of heavy metal ions. We prompted to study the influence of metal ions considering the role of glutathione as detoxification agent in the body. Additionally, the ability of glutathione to complex with metal ions like lead and mercury is well known. We studied the interaction of different metal ions including Pb with the end to end assembled chains of gold nanorods. We found that Pb ions disassembled the chains to dimeric structures. We used high resolution transmission electron microscopy, dynamic light scattering, FTIR and UV-VIS absorption spectroscopy to study the ensemble. Effect of the concentration of Pb ions was also studied and observed a decrease in size of the rods between concentration ranges of 0.1 mM -0.025 mM. We also studied the formation of chain like structures of GNRs induced by L-cysteine. We found that Cu ions selectively disassemble the nano assembly indicating the possibility of generating a new copper sensor. Our data show the feasibility of tuning gold nanorod to form discrete structures in the presence of certain analyte. Our results apparently indicate that analyte induced disassembly is an attractive approach to the detection of clinically and environmentally relevant components.

4.1 Future Prospects

Though we have proved the multisensing of two analytes (e. g. amino acid and metal ion) using gold nanorod by using assembly and disassembly concepts, simultaneous real time monitoring specifically in biological matrices was not done. Future studies will be directed to refine our approach towards this goal.

Bibilography

1 Ali EM, Zheng Y, Yu HH, Ying JY. Ultrasensitive Pb^{2+} detection by glutathione capped quantum dots. Anal. Chem. 2007; 79: 9452-9458.

2 Baker DH. Czarnecki-Maulden GL. Pharmacologic role of cysteine in ameliorating or exacerbating mineral toxicities. J. Nutr. 1987;117:1003-1010.

3 Bala T, Prasad BLV, Sastry M, Kahaly MU, Umesh V, Waghmare UM. Interaction of different metal Ions with carboxylic acid group a quantitative study, J. Phys. Chem. A. 2007; 111: 6183-6190.

4 Ballatori N. Glutathione mercaptides as transport forms of metals. Adv Pharmacol. 1994; 27: 271–298.

5 Banwell CN, Mc Cash EM. Fundamentals of molecular spectroscopy. Mc. Graw- Hill international; 1994:55-98.

6 Bohren DR, Huffman DR. Absorption and scattering of light by small particles. New York Wiley; 1983:35-48.

7 Bourg MC, Badia A, Lennox RB. Gold sulfur bonding in 2D and 3D self-assembled monolayers XPS characterization. J. Phys. Chem. B. 2000; 104: 6562-6567.

8 Caswell KK, Wilson JN, Bunz UHF, Murphy CJ. Preferential end to end assembly of gold nanorods by biotin streptavidin connectors. J. Am. Chem. Soc. 2003; 125: 13914-13915.

9 Chang JY, Wu H, Chen H, Ling YC, Tan W. Oriented assembly of gold nanorods using biorecognition system, Chem. Commun. 2005; 9: 1092–1094.

10 Chang SS, Shih CW, Chen CD, Lai WC, Wang CRC. The shape transition of gold nanorods. Langmuir .1999; 15: 701-709.

11 Clifton JC. Mercury exposure and public health. Pediatr Clin North Am. 2007; 54 : 237–269.

12 Cossaro A, Mazzarello R, Rousseau R, Casalis L, Verdini A, Kohlmeyer A, Floreano L, Scandolo S, Morgante A, Klein ML, Scoles G. X-ray diffraction and computation yield the structure of alkanethiols on gold (111). Science. 2008; 321: 943-946.

13 Dart RC, Hurlbut KM, Boyer-Hassen LV. Lead Medical Toxicology, 3rd edition. Lippincott Williams & Wilkin: 2004. 21-43.

14 Denney RC, Sinclair R. Visible and Ultraviolet Spectroscopy. John Wiley & Sons; 1987: 17-49.

15 Droge W, Holm E. Role of cysteine and glutathione in HIV infection and other diseases associated with muscle wasting and immunological dysfunction. The FASEB Journal. 1997; 11:1077-1089.

16 Durr NJ, Larson T, Smith DK, Korgel BA, Sokolov K, Yaka AB. Two photon luminescence imaging of cancer cells using molecularly targeted gold nanorods, Nano Lett. 2007; 7: 941-945.

17 Egerton RF. Physical Principles of Electron Microscopy An introduction to TEM, SEM and AEM. New York: Springer; 2005: 57-88.

18 El-sayed MA. Some interesting properties of metals confined in time and nanometer space of different shapes. Acc. Chem. Res. 2001; 34: 257–264.

19 Esumi K, Matsuhisa K, Torigoe K. Preparation of rod like gold particles by UV irradiation using cationic micelles as a template. Langmuir. 1995; 11: 3285-3287.

20 Eustis S, El- Sayed MA. Why gold nanoparticles are more precious than pretty gold: Noble metal surface plasmon resonance and its enhancement of the radiative and nonradiative properties of nanocrystals of different shapes, Chem. Soc. Rev. 2006; 35: 209–217.

21 Fava D, Nie Z, Winnik MA, Kumacheva E. Evolution of self assembled structures of polymer terminated gold nanorods in selective solvents. Adv. Mater. 2008; 20: 4318–4322.

22 Franco R, Schoneveld OJ, Pappa A, Panayiotidis MI. The central role of glutathione in the pathophysiology of human diseases. Arch Physiol Biochem. 2007; 113: 234-58.

23 Gole A, Murphy CJ. Biotin streptavidin induced aggregation of gold nanorods tuning rod rod orientation. Langmuir. 2005; 21: 10756-10762.

24 Gole A, Murphy CJ. Seed mediated synthesis of gold nanorods role of the size and nature of the seed. Chem. Mater. 2004; 16: 3633-3640.

25 Grandbois M, Beyer M, Rief M, Schaumann HC, Gaub HE. How strong is a covalent bond. Science. 1999; 283: 1727-1730.

26 Gronbeck H, Curioni A, Andreoni W. Thiols and disulfides on the Au (111) surface the headgroup gold interaction. J. Am. Chem. Soc. 2000; 122: 3839-3842.

27 Grzelczak M, Vermant J, Furst EM, Marza´n LML. Directed Self-Assembly of Nanoparticles. ACS Nano. 2010; in press.

28 Hauck TS, Jennings TL, Yatsenko T, Kumaradas JC. Chan WCW. Enhancing the toxicity of cancer chemotherapeutics with gold nanorod hyperthermia, Adv. Mater. 2008; 20: 3832–3838.

29 Hauck TS, Ghazani AA , Warren C. W. Chan WCW. Assessing the effect of surface chemistry on gold nanorod uptake, toxicity, and gene expression in mammalian cells. Small. 2008; 4: 153-159.

30 http://www.malvern.com/LabEng/technology/dynamic_light_scattering.htm

31 Huang X, El-Sayed IH, Qian W, El-Sayed MA. Cancer cells assemble and align gold nanorods conjugated to antibodies to produce highly enhanced sharp and

polarized surface raman spectra a potential cancer diagnostic marker. Nano Lett. 2007; 7: 1591-1597.

32 Huang X, El-Sayed IH, Qian W, El-Sayed MA. Cancer cell imaging and photothermal therapy in the near infrared region by using gold nanorods. J. AM. CHEM. SOC. 2006; 128: 2115-2120.

33 Jain PK, Eustis S, El-Sayed MA. Plasmon coupling in nanorod assemblies optical absorption discrete dipole approximation simulation and exciton coupling Model. J. Phys. Chem. B. 2006; 110: 18243-18253.

34 Jain PK, Lee KS, El-Sayed IH, El-Sayed MA. Calculated absorption and scattering properties of gold nanoparticles of different size shape and composition applications in biological imaging and biomedicine. J. Phys. Chem. B. 2006; 110: 7238-7248.

35 Jana NR, Gearheart L, Murphy CJ. Wet chemical synthesis of high aspect ratio cylindrical gold nanorods. J. Phys. Chem. B. 2001; 105: 4065-4067.

36 Jana NR, Gearheart L, Murphy CJ. Seed mediated growth approach for shape controlled synthesis of spheroidal and rod like gold nanoparticles using a surfactant template. Adv. Mater. 2001; 13: 1389-1393.

37 Jarup L. Health effects of cadmium exposure a review of the literature and a risk estimate. Scandinavian Journal of Work, Environment and Health. 1998; 24: 11–51.

38 Johnson CJ, Dujardin E, Davis SA, Murphy CJ, Mann S. Growth and form of gold nanorods prepared by seed mediated surfactant directed synthesis. J. Mater. Chem. 2002; 12: 1765-1770.

39 Joseph STS, Ipe BI, Pramod P, and Thomas KG. Gold nanorods to nanochains mechanistic investigations on their longitudinal assembly using a, ? - alkanedithiols and interplasmon coupling. J. Phys. Chem. B. 2006; 110: 150-157.

40 Kerker M. The Scattering of light and other electromagnetic radiation. New York Academic press; 1969: 38-40.

41 Kim F, Song JH, Yang P. Photochemical synthesis of gold nanorods. J. Am. Chem. Soc. 2002; 124: 14316-14317.

42 Kuo WS, Chang CN, Chang YT, Yang MH, Chien YH, Chen SJ, Yeh CS. Gold nanorods in photodynamic therapy as hyperthermia agents and in near infrared optical imaging. Angew. Chem. Int. Ed. 2010; 49: 1 -6.

43 Leontidis E, Kleitou K, Leodidou, TK, Bekiari V, Lianos P. Gold colloids from cationic surfactant solutions1 mechanisms that control particle morphology. Langmuir. 2002; 18: 3659-3668.

44 Li L, Li B. Sensitive and selective detection of cysteine using gold nanoparticles as colorimetric probes. Analyst. 2009; 134: 1361-1365.

45 Link S, El-Sayed MA. Shape and size dependence of radiative, non-radiative and photothermal properties of gold nanocrystals. International Reviews in Physical Chemistry. 2000; 19: 409 - 453.

46 Link S, El-Sayed MA. Size and temperature dependence of the plasmon absorption of colloidal gold nanoparticles. J. Phys. Chem. B. 1999; 103: 4212-4217.

47 Liu AC, Chen DC, Lin CC, Chou HH, Chen CH. Application for cysteine monolayers for electrochemical determination of sub-ppb copper (II); Analytical Chemistry.1999;71: 1549–1552.

48 Liu J, Lu Y. A colorimetric lead biosensor using DNAzyme directed assembly of gold nanoparticles. J. AM. CHEM. SOC. 2003; 125: 6642-6643.

49 Liu J, Veo HC, Vervik-Douki EO, Hagen T, Doniger SJ, Chu DW, Brooks GA, ames BN. Chronically and acutely exercised rats: biomarkers of oxidative stress and endogenous antioxidants. J Appl Physiol. 2000; 89: 21–28.

50 Love JC, Estroff LA, Kriebel JK, Ralph G, Nuzzo RG, Whitesides GM. Self assembled monolayers of thiolates on metals as a form of nanotechnology . Chem. Rev. 2005; 105: 1103-1169.

51 Marinakos SM, Chen S, Chilkoti A. Plasmonic detection of a model analyte in serum by a gold nanorod sensor, Anal. Chem.2007; 79: 5278-5283.

52 Marzan LML. Nanomaterials formation and color. Mater.Today. 2004; 7: 26-31. (b) Jain PK, Huang X, El-Sayed IH, El-Sayed MA. Review of some interesting surface plasmon resonance enhanced properties of noble metal nanoparticles and their applications to biosystems. Plasmonics. 2007; 2:107-118.

53 Murphy CJ, Sau TK, Gole AM, Orendorff CJ, Gao J, Gou L, Hunyadi SE, Li T. Anisotropic metal nanoparticles synthesis assembly andoptical applications. J. Phys. Chem. B. 2005; 109: 13857-13870.

54 Nikoobakht B, El-Sayed MA. Preparation and growth mechanism of gold nanorods using seed mediated growth method. Chem. Mater. 2003; 15: 1957-1962.

55 Nikoobakht B, Wang ZL, El-Sayed MA. Self assembly of gold nanorods; J. Phys. Chem. B. 2000; 104: 8635-8640.

56 Nusz GJ, Marinakos SM, Curry AC, Dahlin A, Höök F, Wax A, Chilkoti A. Label Free Plasmonic Detection of Bio molecular Binding by A Single Gold NanoRod, Anal. Chem. 2008; 80: 984-989.

57 Raj V, Sreenivasan K. Selective detection and estimation of C-reactive protein in serum using surface functionalized gold nano particles. Analytica Chimica Acta. 2010; 662: 186–192.

58 Sau TK, Murphy CJ. Seeded high yield synthesis of short Au nanorods in aqueous solution. Langmuir. 2004; 20: 6414-6420.

59 Sudeep PK, Joseph STS, Thomas GK. Selective detection of cysteine and glutathione using gold nanorod; J. AM. CHEM. SOC. 2005; 127: 6516-6517.

60 Thomas KG, Barazzouk S, Ipe BI, Joseph STS, Kamat PV. Uniaxial plasmon coupling through longitudinal self assembly of gold nanorods. J. Phys. Chem. B. 2004; 108: 13066-13068.

61 Ueno Y, Kizaki M, Nakagiri R, Kamiya T, Sumi H, Osawa T. Dietary glutathione protects rats from diabetic nephropathy and neuropathy. J Nutr. 2002; 132: 897-900.

62 Wang L, Zhu Y, Xu L, Chen W, Kuang H, Liu L, Agarwal A, Xu C, Kotov NA. Side by side and end to end gold nanorod assemblies for environmental toxin sensing. Angew. Chem. Int. Ed. 2010; 49: 1 - 5.

63 Wang XF, Cynader MS. Pyruvate Released by Astrocytes Protects Neurons from Copper-Catalyzed Cysteine Neurotoxicity. J. Neurosci.2001; 21:3322–3331.

64 Wang ZL, Gao RP, Nikoobakht B, El-Sayed MA. Surface reconstruction of the unstable {110} surface in gold nanorods. J. Phys. Chem. B. 2000; 104: 5417-5420.

65 Watt IM. The Principle and Practice of electron Microscopy. New York: Cambridge University press; 1985: 20-31.

66 Wu G, Fang YZ, Yang S, Lupton JR, Turner ND. Glutathione metabolism and its implications for health. J Nutr. 2004; 134: 489-492.

67 Xiao N , Yu C. "Rapid Response and Highly sensitive Noncross-Linking Colorimetric Nitrite Sensor Using 4-Aminothiophenol Modified Gold Nanorods, Anal. Chem. 2010; 82: 3659–3663.

68 Yoosaf K, Ipe BI, Suresh CH, Thomas KG. In situ synthesis of metal nanoparticles and selective naked eye detection of lead ions from aqueous media. J. Phys. Chem. C. 2007; 111: 12839-12847.

69 Yu C, Irudayaraj J. Multiplex biosensor using gold nanorods. Anal. Chem. 2007; 79: 572-579.

70 Yu Y, Chang SS, Lee CL, Wang CRC. Gold nanorods electrochemical synthesis and optical properties. J. Phys. Chem. B. 1997; 101: 6661-6664.

71 Zareie MH, Xu X, Cortie MB. In situ organization of gold nanorods on mixed self assembled monolayer substrates. small. 2007; 3: 139 – 145.